Received: 27 October 2022 | Accepted: 26 January 2023

DOI: 10.1002/ajb2.16143

RESEARCH ARTICLE

American Journal of Botany

A phylogenomic analysis of *Lonicera* and its bearing on the evolution of organ fusion

Mansa Srivastav[1] | Wendy L. Clement[2] | Sven Landrein[3] | Jingbo Zhang[4] | Dianella G. Howarth[4] | Michael J. Donoghue[1]

[1]Department of Ecology and Evolutionary Biology, Yale University, New Haven, Connecticut 06520, USA

[2]Department of Biology, The College of New Jersey, Ewing, New Jersey 08628, USA

[3]Xishuangbanna Tropical Botanical Garden, Chinese Academy of Sciences, Menglun, Mengla, 666303, Yunnan, China

[4]Department of Biological Sciences, St. John's University, Queens, New York 11439, USA

Correspondence

Mansa Srivastav, Department of Ecology and Evolutionary Biology, Yale University, New Haven, Connecticut 06520, USA.
Email: mansa.srivastav@yale.edu

Abstract

Premise: The ~140 species of *Lonicera* are characterized by variously fused leaves, bracteoles, and ovaries, making it a model system for studying the evolution and development of organ fusion. However, previous phylogenetic analyses, based mainly on chloroplast DNA markers, have yielded uncertain and conflicting results. A well-supported phylogeny of *Lonicera* will allow us to trace the evolutionary history of organ fusion.

Methods: We inferred the phylogeny of *Lonicera* using restriction site–associated DNA sequencing (RADSeq), sampling all major clades and 18 of the 23 subsections. This provided the basis for inferring the evolution of five fusion-related traits.

Results: RADSeq data yielded a well-resolved and well-supported phylogeny. The two traditionally recognized subgenera (*Periclymenum* and *Chamaecerasus*), three of the four sections (*Isoxylosteum*, *Coeloxylosteum*, and *Nintooa*), and half of the subsections sampled were recovered as monophyletic. However, the large and heterogeneous section *Isika* was strongly supported as paraphyletic. *Nintooa*, a clade of ~22 mostly vine-forming species, including *L. japonica*, was recovered in a novel position, raising the possibility of cytonuclear discordance. We document the parallel evolution of fused leaves, bracteoles, and ovaries, with rare reversals. Most strikingly, complete cupules, in which four fused bracteoles completely enclose two unfused ovaries, arose at least three times. Surprisingly, these appear to have evolved directly from ancestors with free bracteoles instead of partial cupules.

Conclusions: We provide the most comprehensive and well-supported phylogeny of *Lonicera* to date. Our inference of multiple evolutionary shifts in organ fusion provides a solid foundation for in depth developmental and functional analyses.

KEYWORDS

ancestral character state reconstruction, bracteoles, classification, cupule, cytonuclear discordance, fused ovaries, honeysuckle, parallel evolution, phylogeny, RADSeq

Evolution proceeds through the differentiation of new organs, but also through synorganization and the fusion of existing organs (e.g., Endress, 2006, 2016; Sokoloff et al., 2018; Phillips et al., 2020). Organ fusion has played a key role in the evolutionary history of plants, yielding structures that aid in protection, pollination, dispersal, and, hence, survival and diversification. An excellent example is the fusion of organs subtending the megasporangium in the evolution of the integument of the first seeds (e.g., Long, 1966; Rudall, 2021).

The formation of an "epicalyx" through the fusion of bracts subtending the flower has been studied to a limited degree in the Dipsacaceae, Morinaceae, and *Triplostegia* of the Dipsacales (see Hilger and Hoppe, 1984; Hofman and Göttmann, 1990; Roels and Smets, 1996; Donoghue et al., 2003; Mayer, 2016; Naghiloo and Claßen-Bockhoff, 2017). However, comparable fusions in *Lonicera*, one of the largest clades of Dipsacales, with ~140 species, have received little attention, even though at least half of its members fuse their leaves,

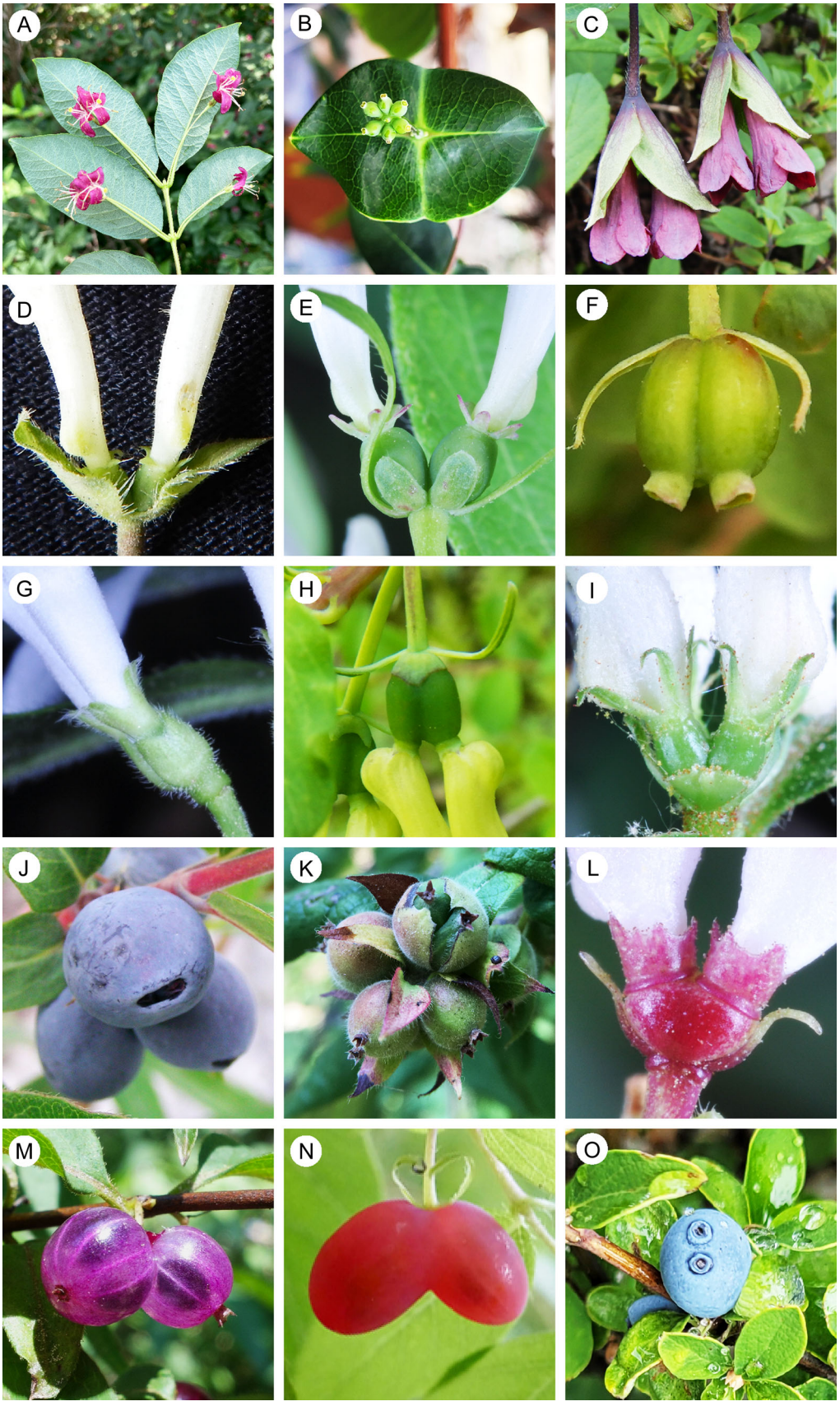

FIGURE 1 (See caption on next page)

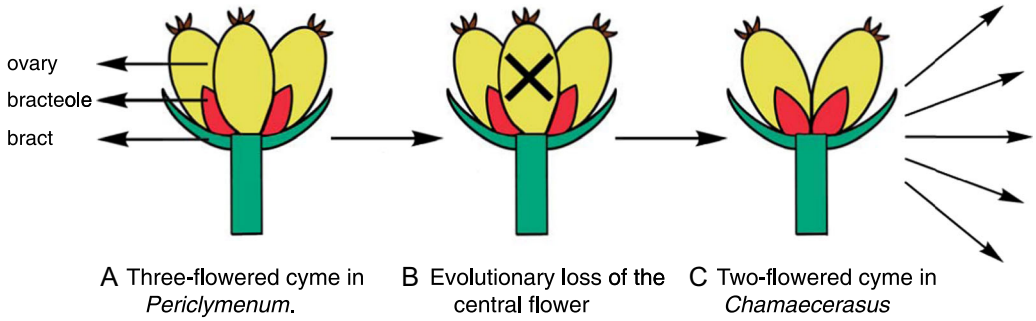

FIGURE 2 (A) The ancestral *Lonicera* cyme is inferred to have had three flowers. This condition is retained in extant species of *Periclymenum*. A pair of bracts (green) subtend the three flowers/ovaries (yellow). Each lateral flower/ovary is subtended by two bracteoles (red; the bracteoles on the opposite side of the two lateral flowers are not shown). (B) The evolutionary loss of the central flower is inferred to have resulted in the derived two-flowered condition. (C) Two-flowered cymes are found today in *Chamaecerasus* species. We hypothesize that the close adjacency of bracteoles and ovaries promoted subsequent evolutionary fusions (arrows denote transitions to various fusion combinations; see Figure 5).

bracts, bracteoles, ovaries, or sometimes even whole flowers (e.g., in some individuals of *L. angustifolia*).

Honeysuckles produce cymes with two or three flowers (Figure 1A, B). In those with three-flowered cymes, two lateral flowers emerge from the axils of the bracteoles of the central flower (Roels and Smets, 1996). The resulting unit has two bracteoles associated with each of the two lateral flowers, along with the two bracteoles of the central flower, which at this later stage are referred to as bracts (Figure 2A). In two-flowered cymes, the central flower is absent and the inferior ovaries of the two lateral flowers are situated right next to one another (Figure 2C). This may have promoted the subsequent evolutionary fusion of the two ovaries to varying degrees. Likewise, the four bracteoles of the two lateral flowers are then positioned close to one another and may fuse in various ways. In some species, all four bracteoles may fuse and form a small cup around the base of the two ovaries. This unit of fused bracteoles can become enlarged and partially or completely enclose the two developing ovaries. In the most derived case, when the four bracteoles are fused and completely enclose the two ovaries, they are said to form a complete cupule. As a complete cupule matures, the ovaries developing inside of it may break out of the cupule (Figure 1K) or mature completely within it (Figure 1J). Through such organ fusions, honeysuckles have evolved entirely new structures that have been integrated with the reproductive apparatus and modified, possibly for purposes of protection or for attracting pollinators or seed dispersers (e.g., as in *L. involucrata*; Burns and Dalen, 2002).

The evolutionary fusion of multiple organs in *Lonicera* provides prime opportunities to investigate the developmental and ecological factors underlying the origin and maintenance of boundaries between organs. However, a major impediment to such studies has been the lack of a comprehensive and confidently resolved phylogeny for *Lonicera*. Here, we report the results of a new phylogenetic analysis of *Lonicera* in which we expand on prior species sampling and use a large restriction site–associated DNA sequencing (RADSeq) data set. We use the resulting phylogenetic framework to evaluate the classification of *Lonicera* and to trace the evolution of organ fusion.

BACKGROUND

In the only worldwide taxonomic treatment of *Lonicera*, which now dates back over a century (Rehder, 1903), honeysuckles were divided into two subgenera, *Periclymenum* and *Chamaecerasus*. In some subsequent treatments, *Periclymenum* has been referred to as *Caprifolium* or as *Lonicera*, and *Chamaecerasus* as *Xylosteum* or as *Lonicera* (Rehder, 1903; Hara, 1983; Hsu and Wang, 1988). Here, for the sake of clarity, we will use Rehder's original names *Periclymenum* and *Chamaecerasus* throughout.

FIGURE 1 The diversity of *Lonicera* reproductive structures, with examples of partially and fully fused organs. Photographs were taken by the authors except as noted. (A) *L. maximowiczii* with two-flowered cymes in the axils of free leaves (photo courtesy of Patrick Sweeney, © 2022 Yale Peabody Museum). (B) *L. sempervirens* showing fused, connate leaves subtending a terminal pair of three-flowered cymes, seen here as six ovaries. (C) *L. porphyrantha* flowers with enlarged bracts surrounding the ovaries. (D) *L. apserifolia* inflorescence with enlarged bracts. (E) *L. tatarica* flowers with free bracteoles and unenlarged bracts (photo courtesy of Patrick Sweeney, © 2022 Yale Peabody Museum). (F) *L. microphylla* with bracteoles absent and fused ovaries. (G) *L. maackii* flower with bracteoles fused within the same flower (photo courtesy of Patrick Sweeney, © 2022 Yale Peabody Museum). (H) *L. obovata* with bracteoles from adjacent flowers fused in pairs. (I) *L. modesta* with all four bracteoles fused into a partial cupule not fully surrounding the ovaries. (J) *L. caerulea* with a complete cupule that is fleshy and blue and entirely encloses a pair of free ovaries within. (K) *L. ferdinandi* infructescence with two free mature ovaries breaking out of a papery, brown complete cupule. (L) *L. gynochlaymdea* flowers with a dark pink, complete cupule tightly enclosing a pair of free ovaries within; the base of the calyx forms a collar-like structure over the opening of the cupule. (M) *L. gynochlamydea* with free translucent-purple ovaries (photo courtesy of Ned Friedman). (N) *L. fragrantissima* with partially fused ovaries (photo courtesy of Elizabeth De Cicco). (O) *L. obovata* with fully fused blue ovaries, similar in appearance to the false fruits of *L. caerulea* (Figure 1J).

Periclymenum contains ~23 species that are mostly vines with terminal inflorescences of three-flowered cymes. The cymes are most often subtended by fused (perfoliate) leaves. By contrast, *Chamaecerasus* contains ~118 species that are mostly shrubs with axillary, two-flowered cymes. Leaves are not fused in *Chamaecerasus*, but flowers and associated structures are very often fused to varying degrees in these species.

Rehder (1903) further divided *Chamaecerasus* into four sections, *Coeloxylosteum*, *Nintooa*, *Isika*, and *Isoxylosteum*. Species of *Coeloxylosteum*, *Nintooa*, and *Isika* have bilateral flowers with one to three nectaries and leaves with convolute leaf vernation. By contrast, *Isoxylosteum* (~4 species) is the only group with radially symmetrical flowers with five nectaries, as well as leaves folded at the midrib in buds. *Coeloxylosteum* (~14 species) is distinguished by hollow stems, and *Nintooa* (~22 species, including the well-known invasive *Lonicera japonica*) by the generally climbing habit. The largest section, *Isika* (~77 species), has no clear synapomorphy.

Rehder further divided the *Chamaecerasus* sections and *Periclymenum* together into 23 subsections based on traits such as bracteole fusion, ovary fusion, fruit color, corolla color, corolla length, corolla symmetry, and bud morphology (Rehder, 1903, 1909, 1913). Since Rehder, there have been several significant regional taxonomic treatments of *Lonicera* (Nakai, 1938; Hara, 1983; Hsu and Wang, 1988; Yang et al., 2011; summarized by Nakaji et al., 2015). These have relied on the same traits emphasized in Rehder's treatments, and fusion traits have figured prominently in all *Lonicera* treatments.

There have been three major molecular phylogenetic analyses of *Lonicera* as a whole, which have used the nuclear ribosomal *ITS* region and five chloroplast markers (Theis et al., 2008; Smith, 2009; Nakaji et al., 2015). These analyses support the monophyly of *Chamaecerasus* and *Periclymenum*, but they differ considerably in regard to relationships within the two major clades. The largest of these analyses (Smith, 2009) included ~55 accepted species and hypothesized that *Lonicera* originated in the Oligocene, likely in Asia, and from there dispersed to temperate forests around the Northern Hemisphere. Two additional studies focused exclusively on *Periclymenum* (Smith and Donoghue, 2010; Zhang and Clement, 2021) and used *ITS*, *LEAFY*, and chloroplast markers. Both found that the subclades of *Periclymenum* sorted geographically rather than according to Rehder's (1903) subsections, with shifts into Mediterranean climates taking place in both Europe and North America.

With the exception of the inclusion of nuclear *ITS* and *LEAFY*, previous phylogenetic analyses have been based on chloroplast DNA data sets. However, a recent study of Dipsacales phylogeny (Lee and Gilman et al., 2021) inferred a tree from hyb-seq data and off-target plastid data collected using the Angiosperms353 probe set. This study included 14 species of *Lonicera* that were not well resolved and differed in trees reconstructed from nuclear exons versus exons plus flanking regions. The plastid trees obtained by Lee and Gilman et al. (2021) largely aligned with previous cpDNA-based analyses, including support for the sister relationship of *Periclymenum* (represented only by *L. periclymenum*) and *Chamaecerasus*.

Despite these past efforts to reconstruct *Lonicera* phylogeny, evolutionary relationships within the two major subclades, *Periclymenum* and *Chamaecerasus*, have not been confidently resolved, which has greatly limited our ability to understand character evolution, and organ fusion in particular.

MATERIALS AND METHODS

Sampling and DNA extraction

Prior phylogenetic work has confidently placed *Lonicera* in the Caprifolioideae clade of Caprifoliaceae, which includes Caprifolieae and *Heptacodium* (Donoghue et al., 2001; Fan et al., 2018; Xiang et al., 2020; Wang et al., 2020; Lee and Gilman et al., 2021). However, relationships among the four major Caprifolieae lineages (*Leycesteria*, *Lonicera*, *Symphoricarpos*, and *Triosteum*) remain unresolved (Lee and Gilman et al., 2021). Here, we included five outgroup species (*Heptacodium miconioides*, *Triosteum himalayanum*, *Leycesteria formosa*, *Symphoricarpos microphyllus*, and *Symphoricarpos oreophilus*) representing all Caprifolioideae lineages, and rooted our trees along the *Heptacodium* branch based on broader phylogenetic analyses (e.g., Lee and Gilman et al., 2021).

We sampled 71 recognized *Lonicera* species (including accessions of nine named entities that are possibly synonymous with other species), or about half of the currently accepted species. We also included a species that resembles *L. angustifolia* but differs in several morphological aspects, here labeled *Lonicera* sp. pending further analyses of the sample. Most of the synonymized entities included here belong to highly morphologically and ecologically variable and geographically widespread species complexes. Specimens referable to sometimes synonymized names were retained in our analyses to check whether they indeed ended up connecting directly with their more broadly accepted counterparts. Their retention also will foster future work on these species complexes, especially given that some were collected in the wild (Appendix 1).

Our sampling covers all four sections of *Chamaecerasus* and 18 of the 23 subsections (Rehder, 1903). We were unable to include five monospecific subsections of *Lonicera*: *Cerasinae*, *Pyrenicae*, *Oblongifoliae*, *Calcaratae*, and *Thoracianthae*. More than one species was sampled for every subsection, except the monospecific ones. Samples were collected from botanical gardens, herbaria, and the wild (Appendix 1). Genomic DNA was extracted using the Beck et al. (2012) modification of the standard CTAB protocol (Doyle and Doyle, 1987). DNA was subsequently cleaned using SpeedBeads (Rohland and Reich, 2012).

Library preparation and data assembly

RADSeq libraries were prepared by Floragenex, Beaverton, Oregon, USA (http://floragenex.com). Samples were digested

using the *Pst*I enzyme followed by adaptor ligation, sonication, end-repair, purification, PCR amplification, and size selection for fragments of length 400–600 base pairs (bp). The average fragment length was 496 bp. The library was sequenced on an Illumina HiSeq. 4000 at the University of Oregon GC3F facility (http://gc3f.uoregon.edu).

We assembled the loci using ipyrad version 0.9.81 (Eaton and Overcast, 2020), with the recently published whole-genome assembly of *Lonicera japonica* (Pu et al., 2020) serving as a reference to exclude possible paralogs (Eaton and Overcast, 2020). We tried different cluster thresholds ranging from 85% to 96%, keeping all other parameters at their default values, and identified the threshold that maximized parsimony informative sites (PIS) and the mean number of loci. We found both to be the highest at 87%, but followed closely by 86%, 95%, 94%, 93%, and 89%.

Simulation and empirical studies have shown that RADSeq data are suitable for inferring phylogenies at deep time scales despite the characteristic large amount of missing data (Rubin et al., 2012; Hou et al., 2015; Leaché et al., 2015; Huang and Knowles, 2016; Eaton et al., 2017; Collins and Hrbek, 2018). However, high proportions of missing data can sometimes erroneously influence phylogenetic inference (Leaché et al., 2015). To explore this, we created 22 data sets with varying amounts of missing data to assess its effect on tree inference. To do so, we fixed the cluster threshold at 87% and varied the minimum number of samples per locus from 4 to 20, 30, 40, 50, 60, and 70. Hereafter, these data sets are referred to as data sets m4 to m20, m30, m40, m50, m60, and m70. Five additional data sets were created by setting cluster thresholds at other values that resulted in a high number of PIS and loci (86%, 93%, 94%, 95%, and 89%) while keeping the minimum number of samples per locus at four.

To understand how the assembly method affected ipyrad statistics and tree inference, we also performed clustering de novo and using a leaf transcriptome of *L. japonica* annotated from the whole genome of *L. japonica* (Pu et al., 2020; https://ngdc.cncb.ac.cn/search/?dbId=gwh&q=+GWHAAZE00000000+). The clustering was done at the minimum number of samples per locus value that maximized bootstrap support values.

Tree inference

Maximum likelihood (ML) trees were inferred using IQ-TREE version 1.6.12 (Nguyen et al., 2015) with 1000 ultrafast bootstrap replicates (Hoang et al., 2018) under the GTR + F + R7 model selected using ModelFinder (Kalyaanamoorthy et al., 2017). Quartet-based trees were reconstructed using Tetrad version 0.9.13 in the ipyrad software (Eaton and Overcast, 2020). Tetrad is a species tree inference program based on the SVDQuartets algorithm (Chifman and Kubatko, 2014). Quartet-based methods are useful for RADSeq data because they allow maximum utilization of the phylogenetic information available for each quartet, irrespective of the amount of missing data in other taxa (Eaton et al., 2017). We inferred trees using the 22 data sets created using the whole genome of *L. japonica* and performed 100 bootstrap replicates, sampling all possible quartets. We also inferred trees for de novo and transcriptome assemblies using IQTree. Figtree version 1.4.4 (Rambaut, 2012) was used to visualize trees, and figures were prepared using the ggtree package (Yu et al., 2017) in R (R Core Team, 2022).

Character scoring

We analyzed five traits, three of which directly concern organ fusion: leaf fusion, bracteole fusion, and ovary fusion. The other two traits—the number of flowers per cyme and enlarged bracts—are related to fusion and have played a major role in *Lonicera* classification. Trait information was assembled from the literature, floras, and herbarium specimens (Appendix S1), as well as from the authors' personal observations in the field and in botanical gardens (Arnold Arboretum of Harvard University; University of California, Berkeley Botanical Garden; University of Washington Botanic Gardens; and Marsh Botanical Garden at Yale University). The morphological character matrix is available in the Dryad Digital Repository (https://datadryad.org/stash/dataset/doi:10.5061/dryad.dv41ns22z; Srivastav et al., 2023). Character states were delimited as follows:

Leaf fusion

(0) Free (Figure 1A) or (1) perfoliate (Figure 1B). Leaves were scored as perfoliate when the opposite leaves fused at their bases around the stem. We followed the scoring of Zhang and Clement (2021), assigning the fused state to those species in which at least the first pair of leaves subtending the inflorescence fuse partially or fully, and the free state to those that do not fuse leaves at all.

Number of flowers per cyme

(0) Three or (1) two. As noted above, species with two flowers lack the central flower of the three-flowered cyme; that is, they produce only the two lateral flowers and their subtending bracteoles. Although *L. gracilipes* is unique (and autapomorphic) in that it most often bears only one flower per cyme, we scored it here as having two flowered cymes on the grounds that this condition is sometimes observed in this species (Hara, 1983). We note also that within *Periclymenum*, flower reduction has been reported in *L. subspicata* var. *subspicata*. However, in this case the loss of the two lateral flowers appears to have resulted in just one central flower per dichasium (Rehder, 1903; Perino, 1978).

Enlarged bracts

(0) Bracts not enlarged (Figure 1E) or (1) bracts enlarged (Figure 1C, D). Species were scored as having enlarged bracts if the bracts were expanded and leaf-like and as long as or longer than the ovaries. Species with bracts that were either not leafy and expanded or leafy and expanded but shorter than the ovaries were scored as not enlarged.

Bracteole fusion

(0) Bracteoles of the lateral flowers present and free from one another (Figure 1E), (1) bracteoles absent or highly reduced (Figure 1F), (2) bracteoles of the same flower fused (Figure 1G), (3) bracteoles of adjacent flowers fused in pairs (Figure 1H), (4) all bracteoles fused into a cup that partially covers the pair of adjacent ovaries (partial cupule; Figure 1I), or (5) all bracteoles fused into a cupule that completely envelops the pair of adjacent ovaries (i.e., a complete cupule; Figure 1J–L).

Ovary fusion

(0) Ovaries free or fused only at the base (less than one-quarter of the mature ovary length; Figure 1M), (1) ovaries partially fused (between one-quarter and three-quarters of the mature ovary length; Figure 1N), or (2) ovaries fully fused (more than three-quarters of the ovary length or fully fused; Figure 1O). This trait was scored using a visual assessment of fruit fusion in matured fruits. The scoring was informed by the observation that when a pair of ovaries are free or partially fused, calyces of the two flowers tend to point away from one another (Figure 1N). By contrast, when a pair of ovaries are fully fused, the two calyces are oriented in parallel, pointing away from the stalk (Figure 1F, O).

Ancestral state reconstruction

Character evolution was traced on an IQTree built using the *L. japonica* reference genome at cluster threshold 87% and a minimum number of samples per locus that would result in the highest bootstrap support values. Prior to performing these analyses, we removed seven tips that are considered synonyms: *L. discolor* and *L. orientalis* = *L. caucasica*; *L. insularis* = *L. morrowii*; *L. hemsleyana* = *L. webbiana*; *L. reticulata* = *L. prolifera*; *L. vesicaria* = *L. ferdinandi*; and *L. inconspicua* = *L. tangutica*. All the synonyms were, in fact, recovered as sisters to their accepted species. *Lonicera tatsiensis* is considered a synonym of *L. webbiana*, but *L. webbiana* could not be sampled, so we retained *L. tatsiensis*. Similarly, *L. lanceolata* is considered a synonym of *L. nigra*, but it was retained because we were unable to sample *L. nigra*.

Maximum parsimony (MP) reconstructions were carried out in Mesquite version 3.61 (Maddison and Maddison, 2018), and ML reconstructions in phytools version 1.0-1 (Revell, 2012). For ML, we tested three models: equal rates (ER), symmetric (SYM), and all rates different (ARD). The best-fit model was determined using AIC scores, AICc scores, and Akaike weights (calculated in the R package qPCR version 4-1; Ritz and Spiess, 2008).

To explore possible phylogenetic correlations between the fusion of ovaries or bracteoles between adjacent flowers and the number of flowers per cyme, we used the fitPagel function in phytools. Likewise, we tested for a correlation between enlarged bracts and bracteole loss, given that many species with enlarged bracts have been described as bracteole-free (Rehder, 1903). In these tests, taxa that were polymorphic for ovary or bracteole fusion were coded as free and those polymorphic for bracteole absence were coded as having bracteoles. We also carried out a "precursor" analysis to test whether the loss of the central flower from the three-flowered cyme promoted subsequent organ fusions using the R package corHMM version 2.7 (Boyko and Beaulieu, 2020).

RESULTS

Ipyrad statistics

We separately assembled RADSeq libraries, using as reference both the whole genome of *L. japonica* and a *L. japonica* leaf transcriptome (Pu et al., 2020). In both cases, the same ingroup tree topologies were recovered, indicating that, given a sufficiently representative transcriptome, the lack of a reference genome is not necessarily an obstacle to reliable assembly.

The whole-genome and transcriptome assemblies generated narrower ranges of ipyrad output statistics than the de novo method. Trees built with the m8 assembly had the highest bootstrap support values. Clustering using the whole genome yielded 3,590,967 bp, 472,092 single-nucleotide polymorphisms (SNPs), 186,213 PIS, ~10,776 mean number of loci, and ~73% missing data. The de novo method resulted in lower values (2,498,181 bp, 335,216 SNPs, 136,804 PIS, and ~7,856 mean number of loci) but a similar amount of missing data (73.06%). The transcriptome assembly yielded the lowest assembly statistics: 1,424,601 bp, 171,476 SNPs, 73,795 PIS, ~6,094 mean number of loci, and ~64% missing data. Details of the ipyrad output are provided in Appendix S2.

Phylogenetic inference

IQTree and Tetrad topologies were largely congruent (Figure 3; Appendix S3). They both recovered two major clades corresponding to Rehder's (1903) two subgenera, *Periclymenum* and *Chamaecerasus*. Sections *Coeloxylosteum*, *Isoxylosteum*, and

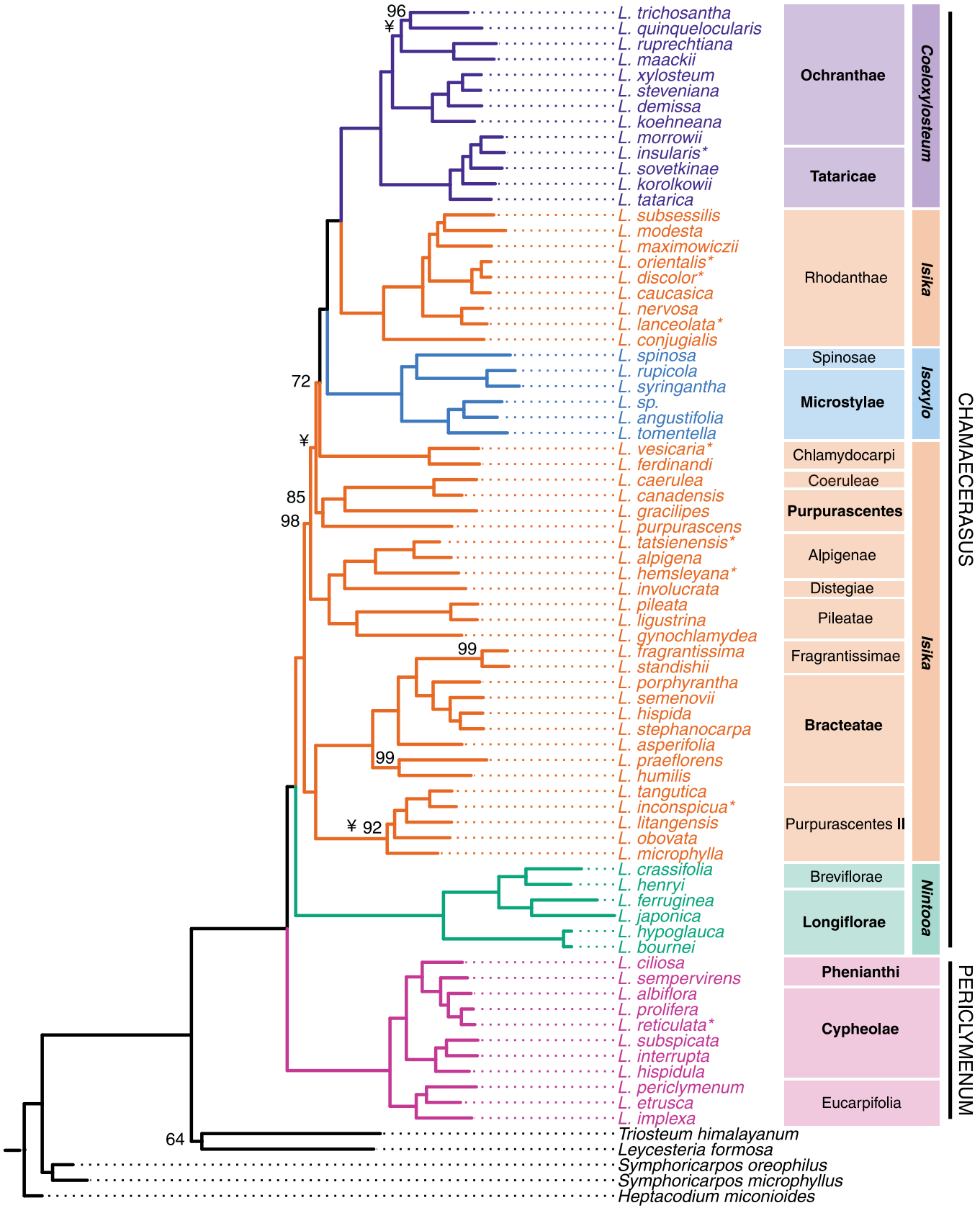

FIGURE 3 Maximum likelihood (IQTree) tree of *Lonicera*. All nodes have ultrafast bootstrap support of 100 unless otherwise noted. *Lonicera* subgenera, sections, and subsections are indicated to the right of the tip names, following the taxonomic treatment of Rehder (1903). Branches are colored to indicate subgenus *Periclymenum* and the four sections of subgenus *Chamaecerasus* (*Isoxylo* = section *Isoxylosteum*). Non-monophyletic subsections are in bold. Possible synonyms are marked by an asterisk. ¥ denotes the three topological differences between concatenated and quartet-based trees (Appendix S3).

Nintooa each formed clades in our trees; by contrast, *Isika* was strongly supported as paraphyletic (Figure 3). We found support for the monophyly of seven of the 18 subsections that we sampled: *Rhodanthae*, *Chlamydocarpi*, *Alpigenae*, *Pileatae*, *Fragrantissimae*, *Eucarpifolia*, and *Breviflorae* (Figure 3). The following eight subsections were found *not* to be monophyletic: *Ochranthae*, *Tataricae*, *Microstylae*, *Purpurascentes*, *Bracteatae*, *Longiflorae*, *Phenianthi*, and *Cypheolae* (Figure 3). The remaining three subsections that we sampled contain just one species each: *Spinosae*, *Coeruleae*, and *Distegiae*. Trees from all analyses are provided in the Dryad Digital Repository (https://doi.org/10.5061/dryad.dv41ns22z; Srivastav et al., 2023).

Comparison of assembly methods

The whole-genome, transcriptome, and de novo assemblies resulted in identical ingroup topologies. Bootstrap support values were highest for the whole-genome assembly and lowest for the transcriptome assembly.

Comparison of IQTree and Tetrad trees

Most of the branches in the IQTree reconstructed from the m8 data set had 100% bootstrap support, while the Tetrad tree generally had lower support values (Figure 3; Appendix S3). There were three topological differences between the IQTree and Tetrad trees, only one of which was supported strongly in both trees (i.e., the position of *L. quinquelocularis*, with bootstrap values >96%). The conflicts involved (1) the position of *L. quinquelocularis*; (2) the positions of *L. obovata* and *L. microphylla*; and (3) the position of the *Chlamydocarpi* clade, here represented by *L. ferdinandi* and *L. vesicaria*. In the IQTree, within *Coeloxylosteum*, *L. quinquelocularis* and *L. trichosantha* form a clade, sister to *L. maackii—L. ruprechtiana* clade. However, in the Tetrad tree, *L. quinquelocularis* is recovered as sister to *L. trichosantha* plus the *L. maackii—L. ruprechtiana* clade. Within the *Purpurascentes II* clade (including *L. tangutica*, *L. inconspicua*, *L. litangensis*, *L. obovata*, and *L. microphylla*), *L. obovata* and *L. microphylla* switch positions in the two trees. Finally, in the IQTree analyses the *Chlamydocarpi* clade is sister to a large clade including *Isoxylosteum*, *Coeloxylosteum*, and the *Rhodanthae* subgroup of section *Isika* (Figure 3). In the Tetrad tree, however, *Chlamydocarpi* is sister to *L. purpurascens* (Appendix S3).

Effects of minimum coverage

To examine the robustness of phylogenetic analyses at different depths of coverage, we generated 22 data sets, varying the minimum coverage threshold at each locus, ranging from four to 70. IQTree topologies remained unchanged in the 14 data sets from m4 through m17. As the number of included loci diminished in the five data sets from m18 to m50, minor changes occurred with respect to the position of the *Chlamydocarpi* clade and *L. quinquelocularis*. Specifically, at m18 and m19, *Chlamydocarpi* was recovered as sister to *L. purpurascens*, a topology identical to the m8 Tetrad topology, except for the switch in positions of *L. obovata* and *L. microphylla*. At m20, *Chlamydocarpi* became sister to all *Chamaecerasus* species except *Nintooa* and the *Fragrantissimae—Bracteatae—Purpurascentes II* clade. At m30, m40, and m50, *Chlamydocarpi* was found to be to sister to the *Purpurascentes—Coeruleae* clade. Regarding *L. quinquelocularis*, at m19, m40, and m50, it was recovered in a sister position to *L. trichosantha* plus the *L. maackii—L. ruprechtiana* clade, as in most Tetrad trees. Finally, major topological changes were observed in the sparsest data sets of m60 and m70.

The topology of Tetrad trees also remained similar up to m50, except for a change along the backbone with respect to the position of *Purpurascentes II* in a handful of data sets. Specifically, in the m6, m9, m13, m20, and m30 data sets, *Purpurascentes II* was recovered as sister to all species of *Chamaecerasus* except those belonging to *Nintooa* and *Bracteatae—Fragrantissimae*. By contrast, in the remaining 15 data sets, it was recovered as sister to only the *Bracteatae—Fragrantissimae* clade. As in our IQTree analyses, major topological changes occurred at m60 and m70.

As with the location of the *Purpurascentes II* clade, the position of *L. purpurascens* also changed in some data sets in the Tetrad analyses. Specifically, in Tetrad trees at m11, m14, and m30, *L. purpurascens* became sister to the *Chlamydocarpi—Coeruleae—Purpurascentes II* clade, instead of being sister to just *Chlamydocarpi*. At m40 and m50, it was positioned as sister to the *Isoxylosteum—Rhodanthae—Coeloxylosteum* clade. Ipyrad output statistics for different values of the minimum number of samples per locus are presented in Appendix S2, Table S2.

Effects of clustering thresholds

Changing the cluster threshold values (87%, 89% 93%, 94%, and 95%) did not affect the ingroup topology in IQTree analyses. For Tetrad trees, the topologies also remained the same except for those at 89% and 95%. At these values, the backbone changed with respect to *Purpurascentes II*; this had a similar effect to changing the coverage threshold in data sets m6, m9, m13, m20, and m30 in the Tetrad reconstructions. Additionally, increasing the clustering thresholds to 95% shifted the position of *L. purpurascens* as in the Tetrad trees at m11, m14, and m30.

Relationship within Caprifolieae

Rooting along the *Heptacodium* branch, the majority of our reconstructions placed *Triosteum* plus *Leycesteria* as sister to *Lonicera*, with this clade, in turn, sister to *Symphoricarpos*. However, at some cluster thresholds and values for

minimum samples per locus in concatenated trees only, *Leycesteria* alone was found to be sister to *Lonicera*, with *Triosteum* sister to that clade. Differences in outgroup topology did not change relationships or the inference of ancestral states within *Lonicera*.

Ancestral state reconstruction

The equal rates model was found to be the best fit for all traits, based on all three criteria (Table 1). MP and ML resulted in similar reconstructions for all five traits (Appendix S4, Figure S1). Our character evolution analyses included outgroups, but these were omitted from Figure 4 to focus on state changes within *Lonicera*; trees including the outgroups are in Appendix S4.

We infer that ancestral *Lonicera* plants had free leaves, free bracteoles, free ovaries, three-flowered cymes, and unenlarged bracts (Figure 4). Our analyses indicate that two-flowered cymes evolved just once at the base of *Chamaecerasus*, while fused leaves evolved at the base of *Periclymenum* followed by two reversals to free leaves. As discussed in detail below, the other three traits showed varying degrees and patterns of homoplasy.

We did not find the fusion of ovaries and bracteoles of adjacent flowers to be significantly correlated with the number of flowers per cyme. Bracteole loss and enlargement of bracts were also not found to be significantly correlated. Precursor analyses to test whether the loss of the central flower promoted fusion between ovaries and bracteoles of adjacent flowers did not favor the precursor model over other models (Appendix S5, Table S1a, b; Appendix S5, Table S2).

DISCUSSION

Our analyses represent a major advance over prior phylogenetic studies (Theis et al., 2008; Smith, 2009; Nakaji et al., 2015) in providing a large nuclear genomic data set. Using RADSeq data, we have generated a confidently resolved phylogeny including ~63 of the 140 species from both of the traditional subgenera, all four sections of *Chamaecerasus*, and 18 of the 23 subsections. Our phylogenetic results provide a strong foundation for the analysis of organ fusion in *Lonicera*.

Phylogeny and taxonomic implications

Our study corroborates previous studies in demonstrating the utility of RADSeq for successfully resolving deeper scale phylogenetic relationships (Leaché et al., 2015; Eaton et al., 2017), in this case spanning at least 20 million years (Lee and Gilman et al., 2021). We confidently infer a basal split separating the *Chamaecerasus* and *Periclymenum* clades, in agreement with Rehder's (1903) taxonomy and previously published trees based largely on plastid data (Theis et al., 2008; Smith, 2009; Nakaji et al. 2015; Liu et al., 2018). Both of these clades are marked by clear-cut apomorphies: fused leaves and the climbing habit in *Periclymenum* and a reduction to a two-flowered cyme in *Chamaecerasus*.

TABLE 1 Comparison of equal rates (ER), symmetrical (SYM), and all-rates-different (ARD) models for the five fusion-related traits.

Trait	Model	*k*	Log-L	AIC	AICc	Akaike weight
Leaf fusion	ER	1	−17.128308	36.25662	34.31544	0.4223188000
	SYM	1	−17.128308	36.25662	34.31544	0.4223188000
	ARD	2	−17.128308	38.25662	35.43309	0.1553624000
Number of flowers per cyme	ER	1	−15.563701	33.12740	31.18623	0.6057533200
	SYM	3	−14.137387	34.27477	30.62772	0.3413088700
	ARD	6	−13.001055	38.00211	32.23740	0.0529378100
Enlarged bracts	ER	1	−26.816480	55.63296	53.69178	0.4223188000
	SYM	1	−26.816480	55.63296	53.69178	0.4223188000
	ARD	2	−26.816480	57.63296	54.80943	0.1553624000
Bracteole fusion	ER	1	−99.016782	200.0336	198.0924	1.000000e + 00
	SYM	36	−92.067160	274.1343	258.3108	8.114046e-17
	ARD	72	−91.365944	362.7319	408.3201	4.682880e-36
Ovary fusion	ER	1	−61.572100	125.1442	123.2030	9.999984e-01
	SYM	15	−60.907497	151.8150	142.4621	1.616250e-06
	ARD	30	−60.726174	181.4523	177.8053	5.927216e-13

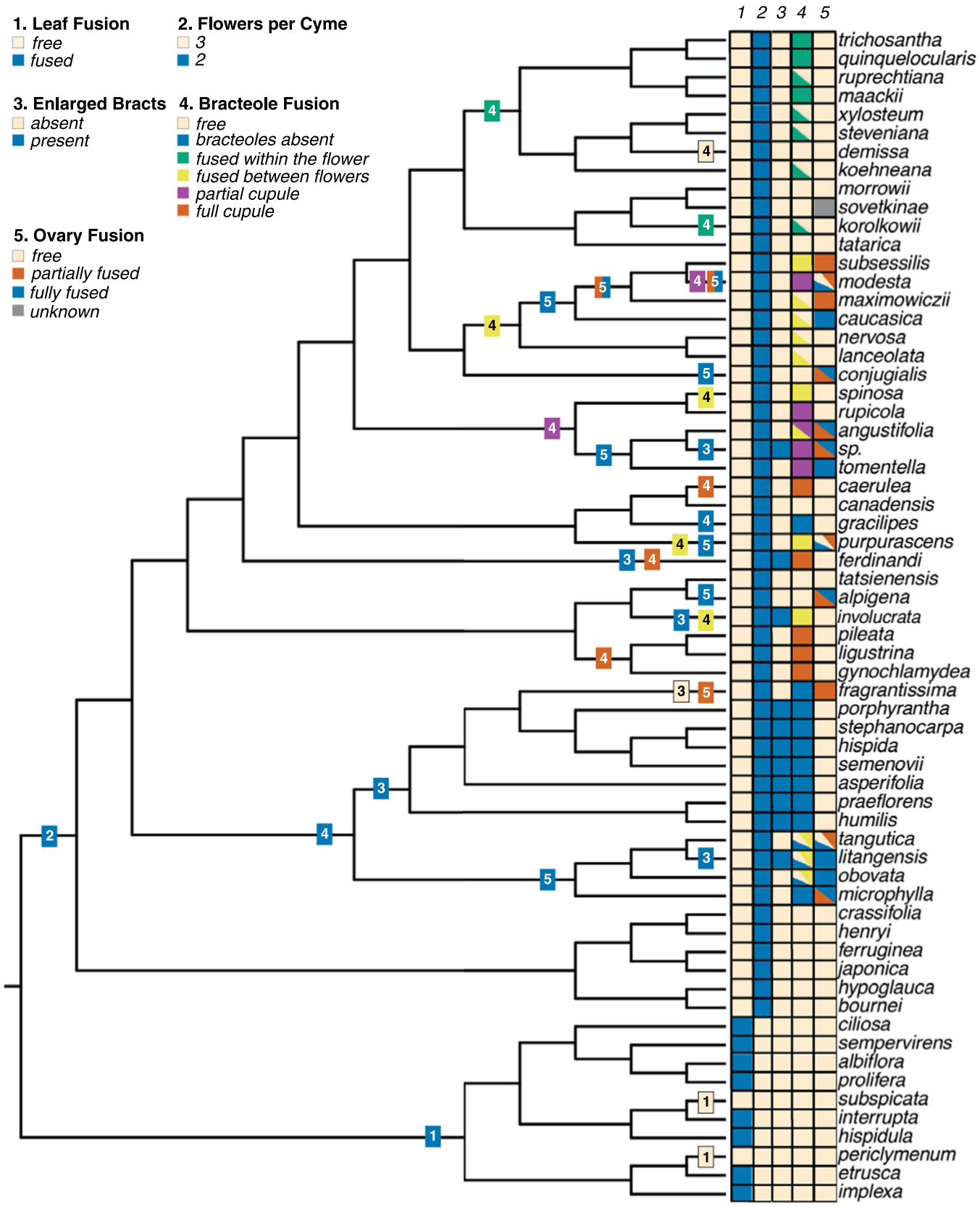

FIGURE 4 (See caption on next page)

As discussed above, changes in the reconstruction method and assembly parameters had very little impact on tree topology or support values. Our discussion will focus on the IQTree obtained using the m8 data set, as this yielded the highest bootstrap support values (Figure 3). Except where noted, the same interpretations hold for all trees.

The topology we recovered for *Periclymenum* is identical to previous studies of that clade (Smith and Donoghue, 2010; Zhang and Clement, 2021), except for relationships within *Eucarpifolia*. Within this clade, our RADSeq analyses find *L. etrusca* to be sister *to L. periclymenum* and this clade to be sister to *L. implexa*. Previous analyses instead found *L. etrusca—L. implexa* to be sister to *L. periclymenum*. We see an early split within *Periclymenum* into a European and a North American clade. Unfortunately, we were unable to sample the Asian species included in previous studies (*L. tragophylla* and *L. subaequalis*), which were shown to form a clade sister to the European–North American clade. Rehder's (1903) largely European subsection *Eucarpifolia* appears to be monophyletic given our sampling, but the North American subsections *Cypheolae* and *Phenianthi* are not monophyletic, although together they form a clade (Figure 3). Within *Cypheolae*, *L. subspicata*, *L. hispidula*, and *L. interrupta* were found to form a clade. Rehder (1903) separated these three species from the remaining species of *Cypheolae* (*L. albiflora*, *L. yunnanensis*, *L. dioica*, *L. glaucescens*, *L. hirsuta*, *L. sullivantii*, and *L. flava*) based on corolla length, gibbous corolla tubes, and bract length. Perino (1978) observed that they also differ from other *Cypheolae* in having pubescent anthers, filament, and stigma, and long inflorescence axes with numerous secondary floral axes (as many as 10 secondary axes, while *L. albiflora*, *L. ciliosa*, *L. reticulata*, and *L. sempervirens* have four at most). The two *Cypheolae* clades recovered here differ in this inflorescence trait.

For *Chamaecerasus*, our RADSeq trees differ substantially from previously published trees. Our study provides strong support for the monophyly of sections *Coeloxylosteum*, *Isoxylosteum*, and *Nintooa* within *Chamaecerasus*. This might have been predicted at the outset, based on the likely derived character states that Rehder associated with the three clades: climbing habit for *Nintooa*, radial flowers for *Isoxylosteum*, and hollow stems for *Coeloxylosteum*. These clades appear to share additional apomorphies. *Nintooa* species also share hollow pith (evolved independently from *Coeloxylosteum*) and black/blue fruits (as opposed to the likely ancestral red fruits). In addition to radial flower symmetry, *Isoxylosteum* is marked by one of the origins of the fusion of bracteoles between flowers. *Coeloxylosteum* species mostly have the two bracteoles of a single flower fused to one another or are polymorphic for this distinctive trait.

Our results confidently reject the monophyly of Rehder's large and heterogeneous section *Isika*, for which we are unable to identify any potential synapomorphies. It is clear that *Isika* must be abandoned, and that a number of previously unrecognized clades should eventually be formally named to better describe the diversity of *Lonicera*. Specifically, we find strong support for a clade including *Isika* subsections *Bracteatae*, *Fragrantissimae*, and most of *Purpurascentes* (here *Purpurascentes II*; Figure 3). This clade shares traits such as the loss of bracteoles (or polymorphism for that trait), as well as flowers with almost radial corolla lobes but a basally bilateral tube. Likewise, *Pileatae*, *Distegiae*, and *Alpigenae* form a well-supported clade. Finally, our analyses highlight that *Isika* subsection *Rhodanthae* is more closely related to *Coeloxylosteum* than it is to the other subsections of *Isika*, a possibility also noted by Nakaji et al. (2015).

A novel placement of *Nintooa*

Here, we recover *Nintooa* in a novel position. Specifically, our analyses strongly support *Nintooa* as sister to all other *Chamaecerasus* species (Figure 3). By contrast, previous analyses placed most species of *Nintooa* in a clade that is nested well within *Chamaecerasus*, sister to a clade comprising *Isoxylosteum*, *Coeloxylosteum*, and *Isika* subsection *Rhodanthae*. Our results imply that the several traits shared by *Nintooa* and *Coeloxylosteum* either are symplesiomorphic (e.g., 4:1 corolla symmetry, unfused ovaries) or have arisen independently in these two lineages (e.g., hollow pith).

We caution, however, that chloroplast and nuclear data strongly support alternative placements of *Nintooa*, and that this could signal a genuine case of cytonuclear discordance (Lee-Yaw et al., 2018). One possibility is that there was admixture early in the history of *Lonicera* between members of the lineages that we now recognize as *Periclymenum* and *Chamaecerasus*. In fact, *Nintooa* species show several traits that appear to bridge the otherwise large morphological gap between *Periclymenum* and *Chamaecerasus*, as Rehder (1903) himself noted. Like *Periclymenum*, *Nintooa* species are mostly vines with a hollow pith, often with terminal inflorescences and long corolla tubes. But, like *Chamaecerasus*, they have

FIGURE 4 Inferred evolutionary transitions for five fusion-related traits, based on maximum likelihood (ML): (1) leaf fusion, two states; (2) number of flowers per cyme, two states; (3) enlarged bracts, two states; (4) bracteole fusion, six states; and (5) ovary fusion, three states. The phylogeny displayed was built with IQTree using the m8 data set after removing the synonyms. Phylogenetic distributions of the states are shown in columns on the right. Polymorphic species for traits 4 and 5 are indicated by two or three colors/states per box. The transitions for these two traits are based on ML analyses in which the polymorphic species were assigned the most derived state (for details, see Appendix S4, Figure S2). Ovary fusion transitions within the *L. caucasica–L. subsessillis* clade were equivocal. Hence, the two transitions within this clade have been depicted with two colors. Outgroups have been removed for illustrative purposes (for reconstructions including outgroups, see Appendix S4).

free leaves and two-flowered cymes. And, intriguingly, *Nintooa* species have been observed to occasionally bear three-flowered cymes, as in *Periclymenum* (Rehder, 1903; Hara, 1983; M. Srivastav, personal observation). We caution that interpretation of the cytonuclear discordance here is complicated by the finding that plastid inheritance can be biparental in *Lonicera* and other Caprifoliaceae (Hu et al., 2008). Finally, it is noteworthy that the branch subtending *Nintooa* is the longest one in our trees. This could also potentially reflect cytonuclear conflict, but may simply indicate an elevated rate of evolution, which, in turn, could impact the tree topology.

Although we were not able to sample it in this study, a related outstanding problem is the placement of *L. calcarata*. It has been widely separated from other *Nintooa* species in previous analyses, appearing to have diverged much earlier in the phylogeny (Theis et al., 2008; Smith, 2009; Nakaji et al., 2015). It is noteworthy that Rehder (1903) placed *L. calcarata* in its own subsection, *Calcaratae*. Unlike any other *Nintooa*, it has fused bracteoles, fused ovaries, and, as its name implies, a long nectar spur (~1.5 cm) unlike any other in *Lonicera* (which, at most, have a gibbous swelling at the base of the corolla tube). It would, therefore, not be surprising if it were distantly related to core *Nintooa*.

Alternative positions for *Purpurascentes II* and *Chlamydocarpi*

In most RADSeq trees, *Purpurascentes II* was found to be sister to the *Fragrantissimae—Bracteatae* clade. Together, these share several potential apomorphies, including (1) the loss of bracteoles and (2) flowers with nearly radial corolla lobes but a bilateral corolla tube. By contrast, previous analyses found *Purpurascentes II* to be sister to all species of *Chamaecerasus* except those belonging to *Bracteatae—Fragrantissimae* and *Nintooa*. This relationship was recovered in only a handful of our Tetrad trees.

Regarding *Chlamydocarpi*, our RADSeq analyses weakly supported it as sister to the *Isoxylosteum—Coeloxylosteum—Rhodanthae* clade, and this entire clade was in turn sister to the *Coeruleae—Purpurascentes* clade. In previous analyses, *Chlamydocarpi* was sister to a much larger clade comprising *Isoxylosteum—Coeloxylosteum—Rhodanthae* along with *Nintooa—Alpigenae—Distegiae—Pileatae—Pyrenicae* (Theis et al., 2008; Smith, 2009; Nakaji et al., 2015). This result was never obtained in our RADSeq analyses.

Subsection-level relationships

With the exception of two monospecific subsections, we sampled all the subsections included in the analyses of Theis et al. (2008). Out of the 18 subsections common to both studies, RADSeq did not support the monophyly of two subsections recovered as clades in their study (*Bracteatae* and *Longiflorae*). This probably reflects the denser sampling of these clades in our study. Conversely, three subsections that were found to be clades in our RADSeq analyses were found to be paraphyletic by Theis et al. (2008). In the case of *Eucarpifolia* they included two species that we did not. *Pileatae* was not monophyletic in their study because *L. gynochlamydea* was separated from the rest (see below). Regarding *Breviflorae*, *L. giraldii* and *L. henryi* were not recovered as sisters, despite their both being considered synonyms of *L. acuminata*.

Smith (2009) sampled 20 subsections, three being monospecific and unsampled in our study. Among the 15 with more than one sampled species, he found only two to be monophyletic. Smith's (2009) tree and our RADSeq trees disagree on the monophyly of five subsections: *Rhodanthae*, *Alpigenae*, *Pileatae*, *Eucarpifolia*, and *Breviflorae*. As in our comparison with the topology of Theis et al. (2008), one source of disagreement could be differences in the species sampled. However, disagreements could also be caused by differences in the specimens used, by possible misidentification, or by genuine conflict between nuclear versus chloroplast genomes. At this stage, it is difficult to sort out these possible causes, but it is noteworthy that our RADSeq results correspond better with the traditional classification of *Lonicera*.

Species-level differences

The most striking species difference was the placement of *L. gynochlamydea*. RADSeq recovered *L. gynochlamydea* within its taxonomic subsection, *Pileatae* (Figure 3), whereas previous analyses found it to be a sister to *Isoxylosteum*. The likely apomorphies of *Pileatae* include translucent purple fruits and a collar-like structure formed by downward extension of the lower section of the calyx tube over the rim of the complete cupule (Figure 1L). It does not share any obvious apomorphies with *Isoxylosteum*. The ranges of *Pileatae* and *Isoxylosteum* do overlap in parts of Hengduan and Himalaya, raising the possibility of discordance due to past introgression.

The other major species-level incongruence concerns the placement of *L. subsessilis*. Our RADSeq analyses recovered it within *Rhodanthae*, where it has been placed traditionally (Rehder, 1903). By contrast, previous analyses found it to be nested deeply within *Coeloxylosteum*, as sister to *L. ruprechtiana*. Like many species of *Rhodanthae*, *L. subsessilis* fuses bracteoles of adjacent flowers. It also has fully fused ovaries, again consistent with a connection to *Rhodanathae*. We know of no apomorphies that might unite *L. subsessilis* with *Coeloxylosteum*. We note that our sample was collected in the wild, whereas other studies have used a specimen from a botanical garden.

Comparison to broader phylogenomic studies

The whole-plastome analyses of Xiang et al. (2020), Fan et al. (2018), and Liu et al. (2018), which focused on

Caprifoliaceae and Dipsacales, also included multiple *Lonicera* species. Their trees match earlier chloroplast studies, but with higher support values, most notably with respect to *Chlamydocarpi* and *Nintooa*, although *L. calcarata* was not sampled. Wang et al. (2020) included a sample of *L. calcarata* and found it to be sister to all other *Chamaecerasus* species with high support, while the remaining *Nintooa* species were nested within *Chamaecerasus*, as in previous chloroplast studies.

The only nuclear phylogenomic study to include multiple *Lonicera* species (Lee and Gilman et al., 2021) yielded results similar to those of our RADSeq tree. This is especially the case in their exon+flanking tree, where, however, many relationships had very low support. Specifically, they recovered *Chlamydocarpi* in the same location as in our RADSeq tree. On the other hand, the placement of the sole *Nintooa* species in their study, *L. henryi*, matched the placement of core *Nintooa* in previous chloroplast trees, though again with very low support.

Overall, our RADSeq data yielded a well-supported phylogeny that aligns better with earlier taxonomic treatments and morphological characters than previous studies. Moving forward, it is imperative to focus special attention on the placement of *Nintooa*, and the very real possibility of ancient hybridization as an explanation for the strong and consistent topological differences between trees based on chloroplast versus nuclear DNA.

The evolution of organ fusion

As noted above, trees obtained using different methods and data sets were substantially similar to one another. Our conclusions regarding character evolution are robust to differences in topology unless otherwise noted. We infer that *Lonicera* started out with free leaves, bracteoles, and ovaries, but these organs were fused in various ways in different lineages.

Leaves fused just once

In agreement with Zhang and Clement (2021), we infer a single transition to perfoliate leaves at the base of *Periclymenum*. Zhang and Clement (2021) hypothesized that fused leaves might aid in the protection of the developing inflorescence or in pollination and seed dispersal by creating a homogeneous background that could increase visibility (also see Perino, 1978). In any case, our analyses also support the finding of Zhang and Clement (2021) that there were two reversals to free leaves within *Periclymenum*, in *L. subspicata* and *L. periclymenum* (Figure 4). The rare *L. griffithii*, which we were unable to sample, is also reported to have free leaves, so this could potentially represent a third reversal. The factors underlying these reversals remain unclear.

Fused bracteoles and cupules evolved multiple times

The evolutionary history of bracteoles has been much more complicated but also shows considerable phylogenetic signal (Figure 4). Ancestrally, we inferred that *Lonicera* had unfused bracteoles (two per flower). This condition was retained in *Periclymenum* (given our present understanding), in *Nintooa*, and along the backbone of the entire tree (Figure 4). Virtually all other bracteole conditions appear to have been derived more or less directly from this ancestral condition (Figures 4 and 5).

One important shift was the loss of bracteoles. A number of species are polymorphic for this trait, which affects our evolutionary interpretation. As shown in Figure 4, if the polymorphic species within *Purpurascentes II* (*L. tangutica*, *L. litangensis*, and *L. obovata*) are scored as lacking bracteoles, then the loss of bracteoles is inferred to have occurred once at the base of the entire *Fragrantissimae—Bracteatae—Purpurascentes II* clade (Appendix S4, Figure S2). In this case, bracteoles would have been regained within the polymorphic species. An alternative interpretation is that bracteoles were lost multiple times, including at the base of the *Fragrantissimae—Bracteatae* clade, in *L. microphylla* of *Purpurascentes II*, and within each of the polymorphic species of that clade (Appendix S4, Figure S1). In either case, bracteoles were lost independently in *L. gracilipes* (Figure 4).

Bracteole fusion in the evolution of *Chamaecerasus* occurred in several different ways. The majority of *Coeloxylosteum* species fuse the two bracteoles of the same flower (Figure 4) or, in the *L. koehneana—L. xylosteum* clade, are polymorphic with free bracteoles (Rehder, 1903). Scoring polymorphic species as having fused bracteoles within flowers (as in Figure 4), ML infers the independent evolution of this condition in *L. korolkowii* and in the *L. trichosantha—L. koehneana* clade (which largely corresponds to subsection *Ochranthae* of Rehder [1903]), and the loss of fused bracteoles in *L. demissa*.

We infer that there were multiple shifts from free bracteoles to the fusion of the bracteoles of two adjacent flowers (Figure 1H, I; Figures 4 and 5). In *Isoxylosteum*, bracteoles of adjacent flowers fuse in pairs in *L. spinosa*, whereas in the other species all four bracteoles fuse to form a small cup surrounding the base of the two ovaries (*L. angustifolia* is polymorphic for the trait). Most *Rhodanthae* species either consistently fuse bracteoles of adjacent flowers or are polymorphic. Similarly, bracteoles of *Purpurascentes II* species may be free, fused between flowers, or lost altogether. Elsewhere in the phylogeny, *L. purpurascens* and *L. involucrata* also exhibit inter-flower bracteole fusion.

An extreme case of bracteole fusion is the formation of a complete cupule, where the four fused bracteoles form a unit that enlarges and completely encloses the two ovaries (Figure 1J–L). Our analyses indicate that this condition evolved at least three times within *Chamaecerasus*: (1) in *Chlamydocarpi*, represented here by *L. ferdinandi*; (2) in

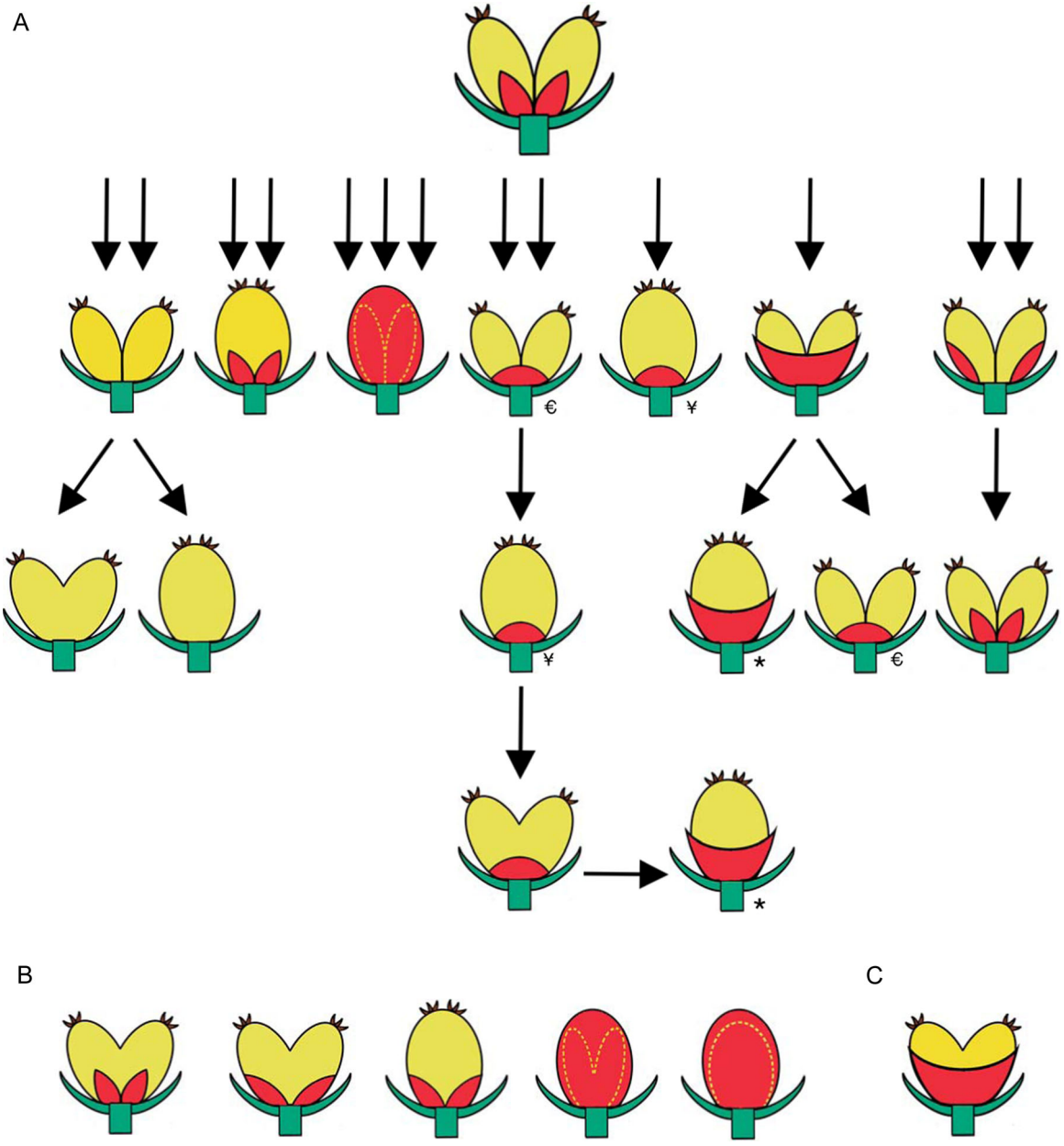

FIGURE 5 (A) Inferred evolutionary transitions to different combinations of bracteole and ovary fusion in *Chamaecerasus*. Each cartoon depicts a particular combination of free or variously fused bracteoles and ovaries. Green = inflorescence stalk and two bracts; these are invariant in these cartoons. Red = bracteoles; when present, there are two per flower/ovary, and these may be fused in various ways (see text); the complete cupule is depicted as a red structure surrounding two developing ovaries within. Yellow = inferior ovary, with the remains of the calyx shown in brown at the apex; ovaries may be free or partially to fully fused. The ancestral condition (free bracteoles and ovaries) is shown at the top. Each arrow denotes an inferred independent transition based on the reconstruction in Figure 4. Among the 18 possible combinations of six bracteole states and two ovary states, 12 are known in extant *Lonicera* species. Convergent evolutions of three bracteole fusion-ovary fusion combinations are marked by *, ¥, and €. (B) Five combinations of bracteole and ovary states that are unknown in extant *Lonicera* species, showing, for example, that fused ovaries are never found in species with a complete cupule. (C) A combination of bracteole and ovary fusion that has not been observed but that could exist, based on observed polymorphisms within some species (i.e., partially fused ovaries surrounded by partial cupule).

Pileatae, in our analyses represented by *L. pileata*, *L. ligustrina*, and *L. gynochlamydea*; and (3) in *L. caerulea*, the single, polyploid species complex comprising *Coeruleae* (Figure 5; Petermann, 1849; Rehder, 1909; Naugžemys et al., 2014).

We note that *Chlamydocarpi* contains three species in addition to *L. ferdinandi*: *L. iberica*, *L. hypoleuca*, and *L. aucherii*. In *L. ferdinandi* and *L. iberica* the cupule is papery and brown at maturity (Figure 1K), and red or orange fruits emerge as they mature. These two species were recovered as sisters by Smith (2009). By contrast, *L. hypoleuca* and *L. aucherii* (which may be synonymous) have a fleshy, hispid, orange-red cupule that later pales to yellow. Neither of these species has ever been sampled, and,

depending on their position in future trees, they could represent an additional origin of a complete cupule.

Our sample of the Asian *Pileatae* clade included all three species. These are marked by a cupule that tightly surrounds the two ovaries at the time of flowering and calyx tissue that extends downward over the lip of the cupule, thus forming a skirt or collar-like structure that completely seals the compartment (Figure 1L). In these species, the ovaries break out of the cupule as they develop and become translucent purple at maturity (Figure 1M).

Lonicera caerulea sensu lato has a circumboreal distribution but also extends south to Central Asia, the Himalayas, and Japan. The cupule of *L. caerulea* turns fleshy and blue (Figure 1J) and completely encloses the (generally blue) ovaries within, through to their maturity (Olmstead, 2019). This "false fruit," which is dispersed as a unit, is especially high in antioxidants and is commercially sold under the name Haskap (Rupasinghe et al., 2012; Celli et al., 2014). This provides an excellent example of the transference of function (Baum and Donoghue, 2002) from the ovary wall to the surrounding cupule. We also note a remarkable case of convergence of dispersal units with a blue color and waxy bloom (Figure 1J, O). In *L. caerulea* this is a cupule that completely envelopes two separate ovaries/fruits within (Figure 1J), whereas in the very similar-looking *L. obovata* there is no cupule and the dispersal unit is formed instead by two completely fused ovaries (Figure 1O).

We were unable to sample the highly unusual Afghanistan-Pakistan endemic *L. griffithii*, which Rehder (1903) placed in his monospecific subsection *Thoracianthae*. But, judging by descriptions and drawings, this seems to represent a completely separate evolution of a cupule-like structure, but within *Periclymenum*. In a clear case of convergent evolution, the bracteoles around the six flowers are fused into a structure that extends out to the length of the ovaries but does not completely close around them. This species deserves very careful study, but so too do other species of *Periclymenum*. Here we have scored all *Periclymenum* species as having free bracteoles, but some degree of organ fusion has been noted (Perino, 1978; J. Zhang, St. John's University, unpublished data). In these species, the bracts and bracteoles are generally very small and very tightly packed, and detailed developmental studies are needed to establish the identity and the nature and extent of fusion of these structures.

Enlarged bracts coincide with bracteole loss

The *Bracteatae—Fragrantissimae* clade is marked by the evolution of enlarged bracts (Figure 4). Bracts are especially well developed in the *Bracteatae* species (Figure 1C, D), and to a lesser extent in *Fragrantissimae*. Bracts in this group may also fuse to a small degree at the base of the two-flowered inflorescence. Bract enlargement generally occurs symmetrically on either side of the inflorescence. Oddly, however, in *L. asperifolia* the bract on one side may enlarge and partially cover the ovaries but be entirely absent from the other side, and one of the bracts is frequently lost or reduced in *L. gracilipes*. Additionally, bracts persist in most species but fall off in *L. oblongifolia* and *L. conjugialis* (Rehder, 1903).

The enlargement of bracts coincides in some fashion with the loss of bracteoles. In the reconstruction shown in Figure 4, bracteoles were lost at the base of the *Fragrantissimae—Bracteatae—Purpurascentes II* clade, and enlarged bracts then evolved in the *Fragrantissimae—Bracteatae* clade, and independently in *L. litangensis* of *Purpurascentes II*. In an alternative reconstruction (shown in Appendix S4, Figure S1), bracteole loss and bract enlargement coincide at the base of the *Fragrantissimae—Bracteatae* clade. In either case, our analyses suggest the possibility that enlarged bracts somehow compensated for the loss of bracteoles (or perhaps vice versa). A phylogenetic correlation test yields an insignificant result, however, as there are too few shifts in these traits in our trees (Appendix S5, Table S1a).

We note that seven of the eleven species with enlarged bracts occupy alpine habitats, where bracts have been shown in other clades to enhance protection from UV radiation, reduce pollen grain wash by rain, and increase flower and fruit temperatures (Song et al., 2013). Outside of the *Bracteatae—Fragrantissimae* clade, *L. involucrata* of western North America also has enlarged bracts that turn red (along with the bracteoles). This creates a strong contrast with the black fruits of this species and has been found to increase fruit consumption rates (Burns and Dalen, 2002).

Ovary fusion evolved multiple times

Unfused ovaries were found to be ancestral in *Lonicera*, from which partially and fully fused ovaries evolved several times (Figures 4 and 5). Not counting shifts within polymorphic species, we infer that unfused ovaries gave rise to partially fused ovaries just once (*L. fragrantissima*) and to fully fused ovaries six times. In one case, partially fused ovaries may have given rise to fully fused ovaries (*L. modesta*), but this conclusion is sensitive to methodological assumptions (see Appendix S4). It is noteworthy that ovary fusion shows more within-species polymorphism than any of the other traits considered here and, when shifts are counted within species, ovary fusion therefore shows the most homoplasy.

Possible drivers of fusion

A major shift in the evolution of *Lonicera* was the single loss of the central flower from the ancestral three-flowered cyme with the origin of *Chamaecerasus* (Figures 2 and 4). This loss has the effect of positioning the two lateral flowers, each with its pair of bracteoles, directly adjacent to one another.

We speculated at the outset that the loss of the middle flower might therefore have served as a "precursor" or "enabler" (*sensu* Donoghue and Sanderson, 2015) for the subsequent fusion of bracteoles and ovaries of the two closely situated flowers. This is consistent with the fact that all well-documented instances of ovary or bracteole fusion between adjacent flowers occur only within *Chamaecerasus* (Figures 4 and 5). Based on our current understanding, there have been at least 14 independent origins of fused bracteoles or fused ovaries between adjacent flowers within *Chamaecerasus* (Figures 4 and 5). Interestingly, such fusions appear not to have taken place in *Nintooa* or *Coeloxylosteum* (where fusions have occurred, but only between the two bracteoles subtending the same flower).

Despite the evident localization of organ fusion between adjacent flowers within the two-flowered clade, we did not find these to be correlated using Pagel tests, likely due to there being just a single origin of the two-flowered condition at the base of *Chamaecerasus* (Appendix S5, Table S1b). In any case, a more appropriate test of our hypothesis is a precursor test (Marazzi et al., 2012; Beaulieu et al., 2013) to determine whether and where in the phylogeny an underlying character (in this case, a shift to the two-flowered cyme) may have promoted the evolution of another trait (the fusion of organs between adjacent flowers). However, here too our data do not fit a precursor model better than they fit conventional models (Appendix S5, Table S2). One explanation is that the loss of the central flower simply did not serve to promote organ fusions. However, it is also possible that our sampling may simply be too limited (i.e., there may be too few tips) to confidently choose among different models (Marazzi et al., 2012; Beaulieu et al., 2013). These tests should be conducted again in the future when the sample has been significantly increased.

Rehder noted that the fusion of organs was correlated with the state of the pith character. Specifically, he commented that the solid-pithed species have a tendency to fuse bracteoles and ovaries of adjacent flowers, whereas in hollow-pithed species, the ovaries never fuse and, at most, only the bracteoles of the same flower unite (specifically in *Coeloxylosteum*). Given that it is hard to imagine a potential mechanistic link between pith development and floral organ fusion, we suspect that hollow pith and bracteole fusion within a flower simply evolved independently in the common ancestor of *Coeloxylosteum* (i.e., "Darwin's scenario"; Maddison and FitzJohn, 2015). In any case, our correlation test did not support a significant connection between these traits (Appendix S5, Table S1c).

Lonicera as a model clade for the study of fusion

Lonicera provides a complex array of organ fusion variation and, hence, could be a model clade for investigating its genetic and developmental bases. As shown in Figures 4 and 5, we have inferred multiple pathways—from the ancestral condition, in which bracteoles and ovaries are free, to the many combinations of fusion that are observed. Surprisingly, these have not always proceeded as one might have expected—for example, in a stepwise fashion from a small degree of fusion of bracteoles to increased fusion and finally to the evolution of a complete cupule. Instead, we mainly see the various derived states originating directly from the ancestral unfused state (Figure 5A). Most unexpectedly, this applies to the three origins of the complete cupule. It would appear that each origin of a cupule arose directly from ancestors with free bracteoles instead of partial cupules, giving us few clues as to how this transition occurred (Figures 4 and 5A). It is possible that we would recover the expected progressive transition series if we added in every species of *Lonicera*, but we suspect that most of the currently unsampled species will be nested within the clades identified here, as opposed to being placed along the stems subtending the cupule-bearing clades. It is also possible that intermediate conditions have been lost through selective extinctions. In any case, we expect that detailed genetic and developmental studies will help resolve this puzzle.

Although many of the possible combinations of bracteole and ovary conditions have evolved, not all of them have (Figure 5B). For example, free, partially fused, and fully fused ovaries can be found in species with bracteoles that are fused to varying degrees between adjacent flowers. By contrast, partially or fully fused ovaries are never found in species in which bracteoles fuse around a single flower or in species with full cupules (Figure 5B). Given the great lability of these traits, it is unclear why some conditions have evolved repeatedly while others appear never to have arisen.

Three other observations deserve further attention. First, although we might expect leaves, bracteoles, and ovaries to be fused in the same species and subclades, fused leaves evolved in a clade in which bracteoles and ovaries are rarely if ever fused. Similarly, bracteole and ovary fusions seem to have originated independently of one another in many cases (Figures 4 and 5). Therefore, while fusion is rampant in *Lonicera*, often only one tissue is fused in any given species. Second, we have inferred only a few cases of reversal, and even these are uncertain (Figure 4; Appendix S4). That is to say, fusion largely appears to have been unidirectional in the evolution of *Lonicera*. Third, polymorphisms within particular species are prevalent in these fusion traits, and it is interesting to note that these polymorphisms themselves show phylogenetic signal. A case in point is the fusion of bracteoles around single flowers in *Coeloxylosteum*. Some species in this clade appear to be fixed for this derived condition, while others have the ability to fuse but have also maintained the development of free bracteoles (Figure 4). The same can be said about species polymorphic for the presence and absence of bracteoles, or for the degree of ovary fusion, in the *Purpurascentes II* clade. Such plasticity within and among related species provides excellent

opportunities to probe the underlying developmental basis of these traits.

It seems likely that the various fusions in *Lonicera* are underlain, at least in part, by a common genetic/developmental mechanism. Fusion and boundary maintenance during meristematic development are governed by a complex gene regulatory network that varies in different plant tissues. However, members of the *CUP SHAPED COTYLEDON* (*NAM/CUC*) subfamily of *NAC* transcription factors have been shown to be involved in boundary separation in nearly all plant tissues across angiosperms (Souer et al., 1996; Aida et al., 1997; Vialette-Guiraud et al., 2011; Phillips et al., 2020). Specifically, it has been found that the loss of the expression of *CUC*-like genes generally leads to more fusion between plant organs, while an increase causes greater separation of tissues in model systems spanning core eudicots.

It is possible that shifts in the regulation of the levels and locations of expression of *CUC* genes could drive much of the fusion found in *Lonicera*. However, it remains to be seen how such changes are localized in separate tissues in different species. Moreover, while *CUC* has been shown to effect plant fusion in nearly all plant tissues, it has not yet been analyzed in rare extrafloral fusions exemplified by *Lonicera*, such as those involving leaves and bracteoles of single or multiple flowers. It is perhaps telling that these extrafloral fusion events occur in a proximal/distal pattern from the ovaries to the leaves subtending inflorescences. This is interesting, given the finding that the levels of auxin, which form a gradient from the tip of a shoot meristem down the shoot axis, modulate *CUC1* and *CUC2* gene expression in *Arabidopsis thaliana* (see Phillips et al., 2020). Additionally, members of the *CUC1/2* clade are also regulated across angiosperms by microRNAs (e.g., miRNA164a, b, and c), which allows for very tight control of *CUC* expression (Vialette-Guiraud et al., 2011; Phillips et al. 2020). In *A. thaliana*, *CUC* acts in a dose-dependent manner, suggesting that not just the location, but also the level of *CUC* expression, is critical in determining boundary formation (Koyama et al., 2010), and that subtle changes in expression could lead to marked differences in which tissues are fused. By virtue of its extraordinary variation and lability, *Lonicera* provides the ideal natural variation necessary to gain a better understanding of the molecular basis of fusion in plants.

Finally, studies are clearly needed to identify the ultimate drivers of organ fusion from the standpoint of fitness. Some hypotheses have been put forward (e.g., leaf fusion; Zhang and Clement, 2021), but these have not yet been critically tested. In other cases, we can only imagine possible roles. Cupules, for example, might aid in fruit dispersal and/or protect the young ovaries from predation, and fused ovaries could enhance seed dispersal. As we have highlighted, *Lonicera* provides the natural variation to design experiments to compare the performance of multiple traits and trait combinations.

AUTHOR CONTRIBUTIONS

M.S. and M.J.D. conceived the study, which was then designed by M.S., W.L.C., and M.J.D. M.S. conducted the lab work and analyses, prepared the figures, and drafted the manuscript. M.J.D., W.L.C., D.G.H., S.L., and J.Z. advised throughout, added information on particular characters, and edited the paper.

ACKNOWLEDGMENTS

The authors thank the members of the honeysuckle working group at the College of New Jersey, St. John's University, and Yale University for valuable discussions that clarified the ideas addressed in the paper. We thank the Biodiversity of the Hengduan Mountains project for providing samples, and the staffs of the Arnold Arboretum of Harvard University, Denver Botanic Gardens, Harvard University Herbaria, New York Botanical Garden, Wildlife Institute of India Herbarium and Library, University of California Botanical Garden at Berkeley, University of Washington Botanical Garden, Xishuangbanna Tropical Botanical Garden, and Yale University Herbarium for helping us acquire material for the study. In this regard, we especially thank H. Forbes, C. Newlander, R. Larson, A. Brach, M. Dosmann, P. Sweeney, and D. Olmstead. We also want to thank Elizabeth De Cicco, Ned Friedman, and Patrick Sweeney for allowing the use of their photographs. Finally, we thank two anonymous reviewers for their very helpful comments. We are very grateful to the National Biodiversity Authority of India for granting collection permits, and to Amit Kumar and G. S. Rawat for helping with collections in India. This work was funded by National Science Foundation grants to M.J.D. (DEB-1929533), W.L.C. (DEB-1929670), and D.G.H. (DEB-1929674), the Macmillan Center at Yale University, and the Yale Institute for Biospheric Studies.

OPEN RESEARCH BADGE

This article has earned an Open Data badge for making publicly available the digitally-shareable data necessary toreproduce the reported results. The data are available at https://doi.org/10.5061/dryad.dv41ns22z. Learn more about the Open Practices badges from the Center for Open Science: https://osf.io/tvyxz/wiki.

DATA AVAILABILITY STATEMENT

All sequences generated for this work are available on NCBI Sequence Read Archive (SRA) under the BioProject PRJNA925902. Alignments, trees, and morphological character matrix are available on the Dryad Digital Repository (https://doi.org/10.5061/dryad.dv41ns22z; Srivastav et al., 2023).

ORCID

Mansa Srivastav http://orcid.org/0000-0002-2531-2137
Wendy L. Clement http://orcid.org/0000-0001-5335-1013
Sven Landrein http://orcid.org/0000-0003-0028-2450
Jingbo Zhang http://orcid.org/0000-0002-5683-9660

Dianella G. Howarth http://orcid.org/0000-0002-9541-7735
Michael J. Donoghue http://orcid.org/0000-0002-2151-4831

REFERENCES

Aida, M., T. Ishida, H. Fukaki, H. Fujisawa, and M. Tasaka. 1997. Genes involved in organ separation in *Arabidopsis*: an analysis of the cup-shaped cotyledon mutant. *Plant Cell* 9: 841–857.

Baum, D. A., and M. J. Donoghue. 2002. Transference of function, heterotopy, and the evolution of plant development. *In* Q. C. B. Cronk, R. M. Bateman, and J. A. Hawkins [eds.], Developmental Genetics and Plant Evolution, 52–69. Taylor and Francis, London, UK.

Beaulieu, J. M., B. C. O'Meara, and M. J. Donoghue. 2013. Identifying hidden rate changes in the evolution of a binary morphological character: the evolution of plant habit in Campanulid Angiosperms. *Systematic Biology* 62: 725–737.

Beck, J. B., P. J. Alexander, L. Allphin, I. A. Al-Shehbaz, C. Rushworth, C. D. Bailey, and M. D. Windham. 2012. Does hybridization drive the transition to asexuality in diploid *Boechera*? *Evolution* 66: 985–995.

Boyko, J. D., and J. M. Beaulieu. 2020. Generalized hidden Markov models for phylogenetic comparative datasets. *Methods in Ecology and Evolution* 12: 468–478.

Burns, K. C., and J. L. Dalen. 2002. Foliage color contrasts and adaptive fruit color variation in a bird-dispersed plant community. *Oikos* 96: 463–469.

Celli, B. G., A. Ghanem, and M. S. L. Brooks. 2014. Haskap berries (*Lonicera caerulea* L.)—a critical review of antioxidant capacity and health-related studies for potential value-added products. *Food and Bioprocess Technology* 7: 1541–1554.

Chifman, J., and L. Kubatko. 2014. Quartet inference from SNP data under the coalescent model. *Bioinformatics* 30: 3317–3324.

Collins, R. A., and T. Hrbek. 2018. An in silico comparison of protocols for dated phylogenomics. *Systematic Biology* 67: 633–650.

Donoghue, M. J., C. D. Bell, and R. C. Winkworth. 2003.The evolution of reproductive of characters in Dipsacales. *International Journal of Plant Sciences* 164: S453–S464.

Donoghue, M. J., T. Eriksson, P. A. Reeves, and R. G. Olmstead. 2001. Phylogeny and phylogenetic taxonomy of Dipsacales, with special reference to *Sinadoxa* and *Tetradoxa* (Adoxaceae). *Harvard Papers in Botany* 6: 459–479.

Donoghue, M. J., and M. J. Sanderson. 2015. Confluence, synnovation, and depauperons in plant diversification. *New Phytologist* 207: 260–274.

Doyle, J., and J. L. Doyle. 1987. Genomic plant DNA preparation from fresh tissue—CTAB method. *Phytochemical Bulletin* 19: 11–15.

Eaton, D. A. R., and I. Overcast. 2020. ipyrad: Interactive assembly and analysis of RADseq datasets. *Bioinformatics* 36: 2592–2594.

Eaton, D. A. R., E. L. Spriggs, B. Park, and M. J. Donoghue. 2017. Misconceptions on missing data in RAD-seq phylogenetics with a deep-scale example from flowering plants. *Systematic Biology* 66: 399–412.

Endress, P. K. 2006. Angiosperm floral evolution: morphological developmental framework. Advances in Botanical Research, vol. 44, 1–61. Academic Press, Cambridge, USA.

Endress, P. K. 2016. Development and evolution of extreme synorganization in angiosperm flowers and diversity: a comparison of Apocynaceae and Orchidaceae. *Annals of Botany* 117: 749–767.

Fan, W.-B., Y. Wu, J. Yang, K. Shahzad, and Z.-H. Li. 2018. Comparative chloroplast genomics of Dipsacales species: insights into sequence variation, adaptive evolution, and phylogenetic relationships. *Frontiers in Plant Science* 9: 689.

Hara, H. 1983. A revision of Caprifoliaceae of Japan with reference to allied plants in other districts and the Adoxaceae. Ginkgoana: contributions to the flora of Asia and the Pacific region, no. 5. Academia Scientific Book Inc., Tokyo, Japan.

Hilger V. H. H., and M. Hoppe. 1984. Die Entwicklung des Aussenkelchs von *Scabiosa*, Sektionen Sclerostemma und Trochocephalus (Dipsacaceae). *Beiträge zur Biologie der Pflanzen* 59: 55–73.

Hoang, D. T., O. Chernomor, A. von Haeseler, B. Q. Minh, and L. S. Vinh. 2018. UFBoot2: Improving the ultrafast bootstrap approximation. *Molecular Biology and Evolution* 35: 518–522.

Hofman, U., and J. Göttmann. 1990. *Morina* L. und *Triplostegia* Wall. ex DC. im Vergleich mit Valerianaceae und Dipsacaceae. *Botanische Jahrbücher für Systematik* 111: 499–553.

Hou, Y., M. D. Nowak, V. Mirré, C. S. Bjorå, C. Brochmann, and M. Popp. 2015. Thousands of RAD-seq loci fully resolve the phylogeny of the highly disjunct arctic-alpine genus *Diapensia* (Diapensiaceae). *PLoS One* 10: e0140175.

Hsu, P. S., and H. J. Wang. 1988. *Lonicera*. *In* P. S. Hsu [ed.], Flora Republicae Popularis Sinicae, 72, 143–259. Beijing: Science Press, China.

Huang, H., and L. L. Knowles. 2016. Unforeseen consequences of excluding missing data from next-generation sequences: simulation study of RAD sequences. *Systematic Biology* 65: 357–365.

Hu, Y., Q. Zhang, G. Rao, and Sodmergen. 2008. Occurrence of plastids in the sperm cells of Caprifoliaceae: Biparental plastid inheritance in Angiosperms is unilaterally derived from maternal inheritance. *Plant and Cell Physiology* 49: 958–968.

Kalyaanamoorthy, S., B. Q. Minh, T. K. F. Wong, A. von Haeseler, and L. S. Jermiin. 2017. Modelfinder: fast model selection for accurate phylogenetic estimates. *Nature Methods* 14: 587–589.

Koyama, T., N. Mitsuda, M. Seki, K. Shinozaki, and M. Ohme-Takagi. 2010. TCP transcription factors regulate the activities of ASYMMETRIC LEAVES1 and miR164, as well as the auxin response, during differentiation of leaves in *Arabidopsis*. *Plant Cell* 22: 3574–3588.

Leaché, A. D., A. S. Chavez, L. N. Jones, J. A. Grummer, A. D. Gottscho, and C. W. Linkem. 2015. Phylogenomics of Phrynosomatid lizards: conflicting signals from Sequence Capture versus Restriction Site Associated DNA sequencing. *Genome Biology and Evolution* 7: 706–719.

Lee, A. K., I. S. Gilman, M. Srivastav, A. D. Lerner, M. J. Donoghue, and W. L. Clement. 2021. Reconstructing Dipsacales phylogeny using Angiosperms353: issues and insights. *American Journal of Botany* 108: 1122–1142.

Lee-Yaw, J. A., C. J. Grassa, S. Joly, R. L. Andrew, and L. H. Rieseberg. 2018. An evaluation of alternative explanations for widespread cytonuclear discordance in annual sunflowers (*Helianthus*). *New Phytologist* 221: 515–526.

Liu, M.-L., W.-B. Fan, N. Wang, P.-B. Dong, T.-T. Zhang, M. Yue, and Z.-H. Li. 2018. Evolutionary analysis of plastid genomes of seven *Lonicera* L. species: implications for sequence divergence and phylogenetic relationships. *International Journal of Molecular Sciences* 19: 4039.

Long, A. G. 1966. XIV.—Some lower carboniferous fructifications from Berwickshire, together with a theoretical account of the evolution of ovules, cupules, and carpels. *Transactions of the Royal Society of Edinburgh* 66: 345–375.

Maddison W. P., and D. R. Maddison. 2018. Mesquite: a modular system for evolutionary analysis, version 3.61. Computer program and documentation distributed by the author. Website: http://www.mesquiteproject.org [accessed 23 October 2022].

Maddison, W. P., and R. G. FitzJohn, 2015. The unsolved challenge to phylogenetic correlation tests for categorical characters. *Systematic Biology* 64: 127–136.

Marazzi, B., C. Ané, M. F. Simon, A. Delgado-Salinas, M. Luckow, and M. J. Sanderson. 2012. Locating evolutionary precursors on a phylogenetic tree. *Evolution* 66: 3918–3930.

Mayer, V. 2016. Dipsacaceae (inclusive *Triplostegia*). *In* Kadereit, J. W., and V. Bittrich [eds.], The Families and Genera of Vascular Plants. Flowering Plants. Eudicots. Aquifoliales, Boraginales, Bruniales, Dipsacales, Escalloniales, Garryales, Paracryphiales, Solanales (except

Convolvulaceae), Icacinaceae, Metteniusaceae, Vahliaceae, vol. 14, 145–163. Springer Nature, Switzerland.
Naghiloo, S., and R. Claßen-Bockhoff. 2017. Developmental changes in time and space promote evolutionary diversification of flowers: A case study in Dipsacoideae. *Frontiers in Plant Science* 8: 1665.
Nakai, T. 1938. A new classification of the genus *Lonicera* in the Japanese empire, together with the diagnoses of new species and new varieties. *The Journal of Japanese Botany* 14: 359–376.
Nakaji, M., N. Tanaka, and T. Sugawara. 2015. A Molecular Phylogenetic Study of *Lonicera* L. (Caprifoliaceae) in Japan Based on Chloroplast DNA Sequences. *Acta Phytotaxonomica et Geobotanica* 66: 137–151.
Naugžemys, D., S. Žilinskaitė, A. Skridaila, and D. Žvingila. 2014. Phylogenetic analysis of the polymorphic 4× species complex *Lonicera caerulea* (Caprifoliaceae) using RAPD markers and noncoding chloroplast DNA sequences. *Biologia* 69: 585–593.
Nguyen, L.-T., H. A. Schmidt, A. von Haeseler, and B. Q. Minh. 2015. IQ-TREE: A fast and effective stochastic algorithm for estimating maximum-likelihood phylogenies. *Molecular Biology and Evolution* 32: 268–274.
Olmstead, S. 2019. Pollinators and pollination of Haskap (Lonicera caerulea L.) in Southern Nova Scotia. M.Sc. dissertation, Dalhousie University, Halifax, Nova Scotia, Canada.
Perino, C. H. 1978. A revision of the genus Lonicera subgenus Periclymenum (Caprifoliaceae) in North America. Ph.D. dissertation, North Carolina State University, Raleigh, USA.
Petermann, W. L. 1849. Deutschlands Flora: it abbildungen sämmtlicher gattungen auf 100 Tafeln, vol. 1. Leipzig, Germany.
Phillips, H. R., J. B. Landis, and C. D. Specht. 2020. Revisiting floral fusion: the evolution and molecular basis of a developmental innovation. *Journal of Experimental Botany* 71: 3390–3404.
Pu, X., Z. Li, Y. Tian, R. Gao, L. Hao, Y. Hu, C. He, et al. 2020. The honeysuckle genome provides insight into the molecular mechanism of carotenoid metabolism underlying dynamic flower coloration. *New Phytologist* 227: 930–943.
R Core Team. 2022. R: A language and environment for statistical computing. R Foundation for Statistical Computing, Vienna, Austria. Website: https://www.R-project.org/ [accessed 23 October 2022].
Rambaut, A. 2012. Figtree v1. 4. Website: http://tree.bio.ed.ac.uk/software/figtree [accessed July 2022].
Rehder, A. 1903. Synopsis of the genus *Lonicera*. *Missouri Botanical Garden Annual Report* 1903: 27–232.
Rehder, A. 1909. Note on the morphology of the fruit of *Lonicera caerulea*. *Rhodora* 11: 209–211.
Rehder, A. 1913. Caprifoliaceae. *In* C. S. Sargent [ed.]. Plantae Wilsonianae: an enumeration of the woody plants collected in western China for the Arborteum of Harvard University during the years 1907, 1908, and 1910, vol. 1, 106–144. Cambridge The University Press, USA.
Revell, L. J. 2012. phytools: an R package for phylogenetic comparative biology (and other things). *Methods in Ecology and Evolution* 3: 217–223.
Ritz, C., and A.-N. Spiess. 2008. qpcR: an R package for sigmoidal model selection in quantitative real-time polymerase chain reaction analysis. *Bioinformatics* 24: 1549–1551.
Roels, P., and E. Smets. 1996. A floral ontogenetic study in the Dipsacales. *International Journal of Plant Sciences* 157: 203–218.
Rohland, N., and D. Reich. 2012. Cost-effective, high-throughput DNA sequencing libraries for multiplexed target capture. *Genome Research* 22: 939–946.
Rubin, B. E. R., R. H. Ree, and C. S. Moreau. 2012. Inferring phylogenies from RAD sequence data. *PLoS One* 7: e33394.
Rudall, P. J. 2021. Evolution and patterning of the ovule in seed plants. *Biological Reviews* 96: 943–960.
Rupasinghe, H. P. V., L. J. Yu, K. S. Bhullar, and B. Bors. 2012. Short Communication: Haskap (*Lonicera caerulea*): A new berry crop with high antioxidant capacity. *Canadian Journal of Plant Science* 92: 1311–1317.
Smith, S. A. 2009. Taking into account phylogenetic and divergence-time uncertainty in a parametric biogeographical analysis of the Northern Hemisphere plant clade Caprifolieae. *Journal of Biogeography* 36: 2324–2337.
Smith, S. A., and M. J. Donoghue. 2010. Combining historical biogeography with niche modeling in the *Caprifolium* clade of *Lonicera* (Caprifoliaceae, Dipsacales). *Systematic Biology* 59: 322–341.
Sokoloff, D. D., M. V. Remizowa, A. C. Timonin, A. A. Oskolski, and M. S. Nuraliev. 2018. Types of organ fusion in angiosperm flowers (with examples from Chloranthaceae, Araliaceae and monocots). *Biologia Serbica* 40: 16–46.
Song, B., Z-Q. Zhang, J. Stöcklin, Y. Yang, Y. Niu, J.-G. Chen, and H. Sun. 2013. Multifunctional bracts enhance plant fitness during flowering and seed development in *Rheum nobile* (Polygonaceae), a giant herb endemic to the high Himalayas. *Oecologia* 172: 359–370.
Souer, E., A. van Houwelingen, D. Kloos, J. Mol, and R. Koes. 1996. The no apical meristem gene of *Petunia* is required for pattern formation in embryos and flowers and is expressed at meristem and primordia boundaries. *Cell* 85: 159–170.
Srivastav, M., W. L. Clement, S. Landrein, J. Zhang, D. G. Howarth, and M. J. Donoghue. 2023. Data from: A phylogenomic analysis of Lonicera and its bearing on the evolution of organ fusion. *Dryad Digital Repository* https://orcid.org/0000-0002-2531-2137.
Theis, N., M. J. Donoghue, and J. Li. 2008. Phylogenetics of the Caprifolieae and *Lonicera* (Dipsacales) based on nuclear and chloroplast DNA sequences. *Systematic Botany* 33: 776–783.
Thiers, B. 2017. [continuously updated] Index Herbariorum: a global directory of public herbaria and associated staff. New York Botanical Garden's Virtual Herbarium. Website: http://sweetgum.nybg.org/science/ih/ [accessed October 2022].
Vialette-Guiraud, A. C. M., H. Adam, C. Finet, S. Jasinski, S. Jouannic, and C. P. Scutt. 2011. Insights from ANA-grade angiosperms into the early evolution of *CUP-SHAPED COTYLEDON* genes. *Annals of Botany* 107: 1511–1519.
Wang, H.-X., H. Liu, M. J. Moore, S. Landrein, B. Liu, Z.-X. Zhu, and H.-F. Wang. 2020. Plastid phylogenomic insights into the evolution of the Caprifoliaceae s.l. (Dipsacales). *Molecular Phylogenetics and Evolution* 142: 106641.
Xiang, C.-L., H.-J. Dong, S. Landrein, F. Zhao, W.-B. Yu, D. E. Soltis, P. S. Soltis, et al. 2020. Revisiting the phylogeny of Dipsacales: new insights from phylogenomic analyses of complete plastomic sequences. *Journal of Systematics and Evolution* 58: 103–117.
Yang, Q., S. Landrein, J. Osborne, and R. Borosova. 2011. Caprifoliaceae. *In* Z. Y. Wu, P. H. Raven, and D. Y. Hong [eds.], Flora of China, vol. 19, 616–641. Science Press, Beijing, China and Missouri Botanical Garden Press, St. Louis, USA.
Yu, G., D. K. Smith, H. Zhu, Y. Guan, and T. T.-Y. Lam. 2017. GGTREE: an R package for visualization and annotation of phylogenetic trees with their covariates and other associated data. *Methods in Ecology and Evolution* 8: 28–36.
Zhang, L., and W. L. Clement. 2021. Evolution of leaf fusion in honeysuckle (*Periclymenum*, *Lonicera*). *International Journal of Plant Sciences* 182: 663–681.

SUPPORTING INFORMATION

Additional supporting information can be found online in the Supporting Information section at the end of this article.

APPENDIX S1. Sources for character scoring.

APPENDIX S2. Ipyrad statistics.

APPENDIX S3. Quartet-based (Tetrad) tree.

APPENDIX S4. Ancestral state reconstruction in maximum likelihood and maximum parsimony frameworks with outgroups included.

APPENDIX S5. Test results for correlation and precursor analyses.

How to cite this article: Srivastav, M., W. L. Clement, S. Landrein, J. Zhang, D. G. Howarth, and M. J. Donoghue. 2023. A phylogenomic analysis of *Lonicera* and its bearing on the evolution of organ fusion. *American Journal of Botany* 110(4): e16143. https://doi.org/10.1002/ajb2.16143

APPENDIX 1: SPECIMEN VOUCHER INFORMATION

For each accession, collector number, collector, and herbarium or living collection information is provided. The Arnold Arboretum of Harvard University, University of California Botanical Garden at Berkeley, University of Washington Botanic Gardens, Xishuangbanna Tropical Botanical Garden, and the Biodiversity of the Hengduan Mountains project (http://hengduan.huh.harvard.edu/fieldnotes) are abbreviated as AA, UCBG, UWBG, XTBG, and Hengduan, respectively. Species are arranged alphabetically. Index Herbariorum (Thiers, 2017) abbreviations are used for herbaria.

Outgroup: ***Heptacodium miconioides*** Rehder: 1549-80*C, living collections, AA; ***Leycesteria formosa*** Wall.: 360-2015*H, living collections, AA; ***Symphoricarpos oreophilus*** A. Gray: 101147, living collections, Denver Botanic Gardens; ***Symphoricarpos microphyllus*** Kunth: 74-0249, living collections, UCBG; ***Triosteum himalayanum*** Wall.: 32623, Hengduan.

Ingroup: ***L. albiflora*** Torr. & A. Gray: 97.0474, living collections, UCBG; ***L. alpigena*** **forma** ***nana*** L.: 1310-84*A, living collections, AA; ***L. angustifolia*** Wall. ex DC.: WII.21209, Mansa Srivastav, WII; ***L. asperifolia*** Hook.f. & Thomson: WII.21204, Mansa Srivastav, WII; ***L. bournei*** Hemsl. ex F. B. Forbes & Hemsl.: 00.2007 0027, living collections, XTBG; ***L. caerulea*** **var**. ***altaica*** L.: 249-96*B, living collections, AA; ***L. canadensis*** Bartram & W. Bartram ex Marshall: NY01283807, New York Botanical Garden DNA Bank; ***L. caucasica*** Pall.: NY01120718, New York Botanical Garden DNA Bank; ***L. ciliosa*** Poir.: 2006.0236, living collections, UCBG; ***L. conjugialis*** Kellogg: 258-08*I, living collections, UWBG; ***L. crassifolia*** Batalin: 2008.068, living collections, UCBG; ***L. demissa*** Rehder: 975-72*A, living collections, AA; ***L. discolor*** Lindl.: 71-17*C, living collections, UWBG; ***L. etrusca*** Santi: 543-93*A, living collections, AA; ***L. ferdinandi*** Franch.: 18169*A, living collections, AA; ***L. ferruginea*** Rehder: 00.2007 0230, living collections, XTBG; ***L. fragrantissima*** Lindl. & Paxton: 286-52*A, living collections, UWBG; ***L. gracilipes*** **forma** ***glabra*** Miq.: 97.0306, living collections, UCBG; ***L. gynochlamydea*** Hemsl.: 80.1447, living collections, UCBG; ***L. hemsleyana*** Rehder: 124-99*B, living collections, AA; ***L. henryi*** Hemsl. ex F. B. Forbes & Hemsl.: 1047-45*A, living collections, UWBG; ***L. hispida*** Pall. ex Schult.: 38596, Hengduan; ***L. hispidula*** Douglas ex Torr. & A. Gray: no accession no., living collections, UWBG; ***L. humilis*** Kar. & Kir.:YU.254960, Young-Ho Ha, Hyh42-1, YU; ***L. hypoglauca*** Miq.: 00.2009 0439, living collections, XTBG; ***L. implexa*** Aiton: 2002.0823, living collections, UCBG; ***L. inconspicua*** Batalin: 34119, Hengduan; ***L. insularis*** Nakai: 73-17*A, living collections, UWBG; ***L. interrupta*** Benth.: 88.0629, living collections, UCBG; ***L. involucrata*** Banks ex Spreng.: 82.1349, living collections, UCBG; ***L. japonica*** Thunb.: 99.0542, living collections, UCBG; ***L. koehneana*** Rehder: 815-84*A, living collections, AA; ***L. korolkowii*** Stapf: 10083-2*A, living collections, AA; ***L. lanceolata*** Wall.: 37137, Hengduan; ***L. ligustrina*** **var**. ***yunnanesis*** A. Gray: 280-2015*B, living collections, AA; ***L. litangensis*** Batalin: 37340, Hengduan; ***L. maackii*** Maxim.: 7190-B, living collections, AA; ***L. maximowiczii*** Regel: YU.254959, Sabeom Jang, Gil2999, YU; ***L. microphylla*** Willd. ex Schult.: WII.21205, Mansa Srivastav, WII; ***L. modesta*** **var**. ***lushanensis*** Rehder: 14-87*B, living collections, AA; ***L. morrowii*** A. Gray: 525-84*A, living collections, AA; ***L. nervosa*** Maxim.: 95-81*D, living collections, AA; ***L. obovata*** Royle ex Hook. f. & Thomson: WII.21203, Mansa Srivastav, WII; ***L. orientalis*** **var**. ***longifolia*** Lam.: 1240-84*A, living collections, AA; ***L. periclymenum*** L.: no accession no., living collections, AA; ***L. pileata*** Oliv.: no accession no., living collections, UCBG; ***L. porphyrantha*** M. P. Nayar & G. S. Giri: WII.21208, Mansa Srivastav, WII; ***L. praeflorens*** Batalin: 657-26*A, living collections, AA; ***L. prolifera*** Rehder: 93.1128, living collections, UCBG; ***L. purpurascens*** Walp.: 216-17*A, living collections, UWBG; ***L. quinquelocularis*** Hardw.: WII.21210 Mansa Srivastav, WII; ***L. reticulata*** Raf.: no accession no., living collections, Denver Botanic Gardens; ***L. rupicola*** **subsp**. ***rupicola*** Hook. f. & Thomson: 44775, Hengduan; ***L. rupicola*** **subsp**. ***syringantha*** Maxim.: 40196, Hengduan; ***L. ruprechtiana*** Regel: 694-88*C, living collections, AA; ***L. semenovii*** Regel: WII.21202, Mansa Srivastav, WII; ***L. sempervirens*** L.: 393-96*A, living collections, AA; ***L. sovetkinae*** Tkatsch.: 796-74*A, living collections, AA; ***L. sp.***: WII.21207, Mansa Srivastav, WII; ***L. spinosa*** Jacquem. ex Walp.: WII.21201, Mansa Srivastav, WII; ***L. standishii*** Jacques: 860-82*A, living collections, AA; ***L. stephanocarpa*** Franch.:32685, Hengduan; ***L. steveniana*** Fisch. ex Pojark.: 694-83*B, living collections, AA; ***L. subsessilis*** Rehder: YU.254958, Sabeom Jang, Gil3000, YU; ***L. subspicata*** **var**. ***subspicata*** Hook. & Arn.: 2004.0105, living collections, UCBG; ***L. tangutica*** Maxim.: 44855, Hengduan; ***L. tatarica*** L.: 299-78*A, living collections, AA; ***L. tatsiensis*** Franch.: 32609, Hengduan; ***L. tomentella*** Hook. f. & Thomson: WII.21206, Mansa Srivastav, WII; ***L. trichosantha*** Bureau & Franch.: 41884, Hengduan; ***L. vesicaria*** Kom.: 184-84*B, living collections, UWBG; ***L. xylosteum*** L.: 856-84*A, living collections, AA.